Supporting Info file

for

Synthesis and Characterization of Carbonyl Functionalized Organotellurium(IV) Derivatives

Puspendra Singh,[*a] Mariya Khan,[b] Andrew Duthie,[c] Ray J. Butcher[d]

[a]Department of Chemistry, Dr. Shakuntala Misra National Rehabilitation University, Lucknow, 226017, India.

[b]Department of Chemistry, University of Lucknow, Lucknow, 226007, India.

[c]Department of Chemistry, Indian Institute of Technology Kanpur, Kanpur, 208016, India

[d]Department of Chemistry, Howard University, Washington DC20059, USA

*Corresponding Author, E-mail address: pushpendrasingh0612@gmail.com

INDEX

Table S1. Crystal Data and Structure Refinement Details of 1, 4 and 5

	1	4	5
empirical formula	$C_{16}H_{14}Cl_2O_2Te$	$C_{19}H_{20}Cl_2O_2Te$	$C_{14}H_{18}Cl_2O_2Te$
formula mass (g mol^{-1})	436.77	478.85	416.78
Temp (K)	100(2)	123(2)	100(2)
Wavelength, λ (Å)	0.710 73	0.710 73	0.710 73
cryst syst	monoclinic	monoclinic	monoclinic
cryst size (mm^3)	0.55 x 0.10 x 0.09	0.77 x 0.55 x 0.35	0.44 x 0.27 x 0.23
space group	$P2_1/c$	$P2_1/c$	$P2_1$
a (Å)	13.395(3)	8.7845(4)	8.389(5)
b (Å)	13.251(3)	19.5434(8)	12.312(5)
c (Å)	9.036(2)	11.0751(5)	8.461(5)
α (deg)	90	90	90.000(5)
β (deg)	98.213(4)	97.679(4)	116.320(5)
γ (deg)	90	90	90.000(5)
Volume (Å^3)	1587.5(7)	1884.3(1)	783.3(7)
Z	4	4	2
ρ_{calcd} (Mg m^3)	1.827	1.688	1.767
abs coeff (mm^{-1})	2.211	1.871	2.235
F(000)	848	944	408
θ range (deg)	2.17-32.17	3.13-40.86	2.69-41.13
index ranges	-19 ≤ h ≤ 18, -18 ≤ k ≤ 19, -13 ≤ l ≤ 12	-15 ≤ h ≤ 16, -35 ≤ k ≤ 27, -20 ≤ l ≤ 19	-14 ≤ h ≤ 15, -22 ≤ k ≤ 22, -15 ≤ l ≤ 11
no. of rflns collected	12748	24302	11130
no. of indep rflns	5046 (*R*(int) = 0.0344)	11990 (*R*(int) = 0.0256)	7370 (*R*(int) = 0.0295)
completeness to *θ*max (%)	99.4	99.8	99.5
abs cor	semiempirical from equivalents	analytical	analytical
max. min. transmission	0.7464, 0.4720	0.593, 0.434	0.733, 0.564
refinement method	full-matrix least squares on F^2	full-matrix least squares on F^2	full-matrix least squares on F^2
No. of data/restraints/ parameters	5046/0/194	11990/0/224	7370/1/179
goodness of fit on F^2	1.040	1.088	1.019
final *R* indices [$I > 2\sigma(I)$]	R1 = 0.0224, wR2 = 0.0570	R1 = 0.0345, wR2 = 0.0652	R1 = 0.0292, wR2 = 0.0569
R indices (all data)	R1 = 0.0255, wR2 = 0.0586	R1 = 0.0515, wR2 = 0.0707	R1 = 0.0344, wR2 = 0.0601
largest diff peak/hole (e Å^{-3})	1.013/-0.549	0.687/-1.097	1.285/-0.985

Table S2. Hydrogen bonds for **1**, **4** and **5** (Å and °).

	D-H···A	**d(D-H)**	**d(H···A)**	**d(D···A)**	**∠(DHA)**	**Symmetry**
1	O(2)-H(2)···O(1)	0.80(3)	1.824(3)	2.559(2)	154(3)	
	C(9)-H(9A)···Cl(1)	0.95	2.667(1)	3.541(2)	153.1	x,-y+1/2,z-1/2
	C(6)-H(5A)···Cl(1)	0.95	2.785(1)	3.261(2)	111.9	-1+x, 0.5-y, -1.5+z
	C(9)-H(9A)···Cl(1)	0.95	2.667(1)	3.541(2)	153.1	1-x, 0.5+y, 0.5-z
	C(15)-H(15A)···Cl(2)	0.95	2.861(1)	3.783(2)	163.7	-1-x, y, -1+z
	C(2)-H(2A)···Cl(2)	0.95	2.853(1)	3.302(2)	110.1	1-x, 1-y, 1+z
	C(13)-H(13A)···O(1)	0.95	2.427(1)	3.339(2)	160.9	1-x, 1-y, 1-z
4	O(2)-H(2)···O(1)	0.75(2)	1.854(2)	2.541(1)	151(3)	
	O(2)-H(2)···O(1)	0.75(2)	2.419(2)	2.884(2)	121(2)	-x+1,-y+1,-z+1
	C(9)-H(9B)···Cl(2)	0.98	2.881(0)	3.629(2)	133.8	1 -x, 1-y. 1-z
	C(7)-H(7B)···Cl(1)	0.98	2.956(0)	3.741(2)	137.9	1 -x, 1-y. 1-z
	C(17)-H(17A)···Cl(1)	0.95	2.902(0)	3.717(2)	144.6	1 -x, 1-y. 1-z
5	O(2)-H(2)···O(1)	0.84	1.744(3)	2.498(3)	148.4	
	C(12)-H(12)···Cl(2)	0.95	2.911(1)	3.704(3)	141.8	1 -x+1,y-1/2,-z+1
	C(7)-H(7B)···Cl(2)	0.95	2.695(1)	3.531(3)	143.6	1-x, -0.5+y, 2-z
	C(14)-H(14A)···O(1)	0.98	2.522(2)	3.501(4)	176.4	-x+1,y-1/2,-z
	C(14)-H(14B)···Cl(1)	0.98	2.843(1)	3.803(4)	166.8	-x+2,y-1/2,-z+1
	C(9)-H(9A)···Cl(1)	0.98	2.872(1)	3.749(3)	149.6	-x+2,y-1/2,-z+1
	C(9)-H(9C)···Cl(1)	0.98	2.778(1)	3.462(3)	127.5	-x+2,y-1/2,-z+1

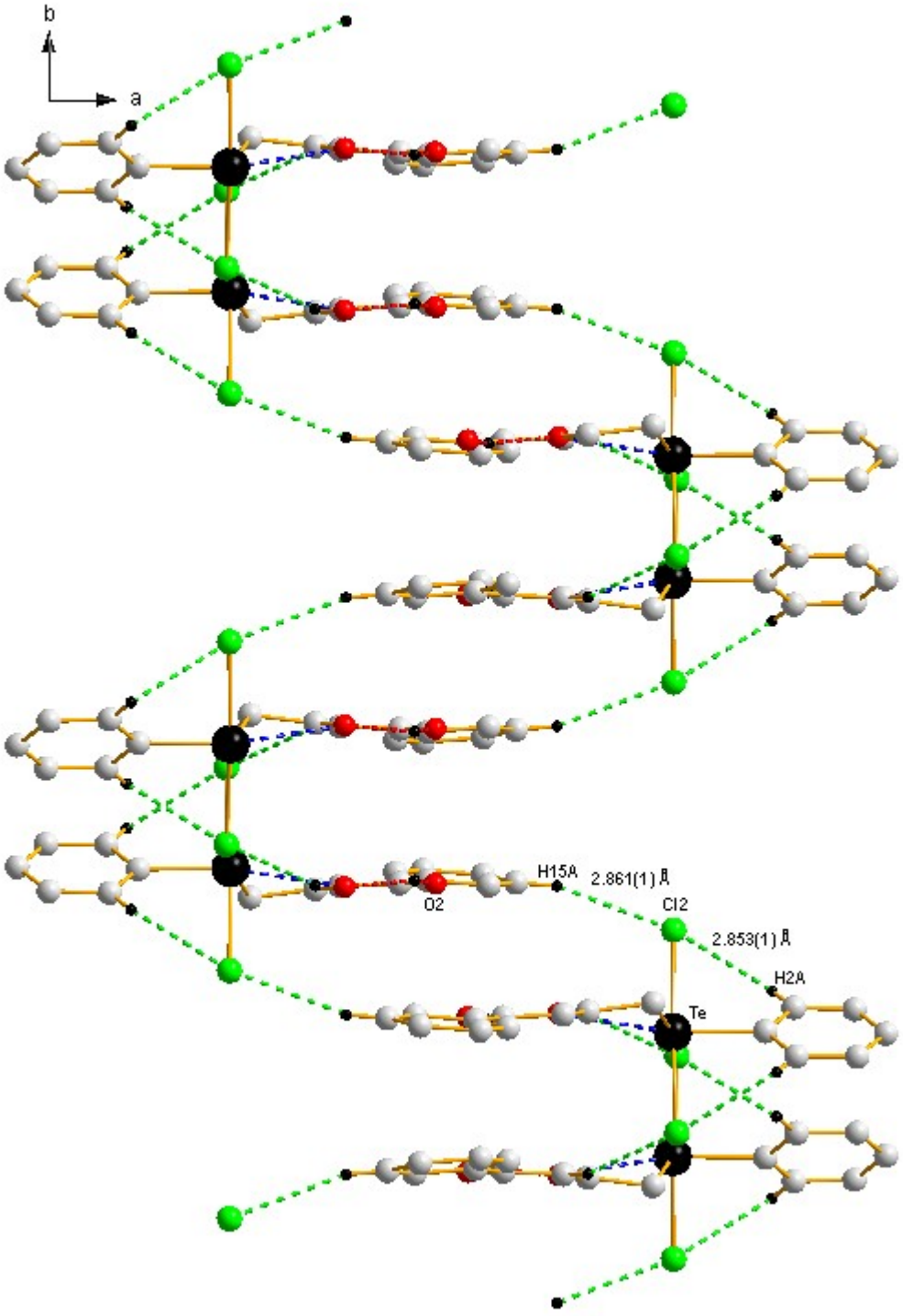

Fig. S1 Crystal lattices of compound **1** showing helical structure through C-H---Cl (green) hydrogen bonding interactions.

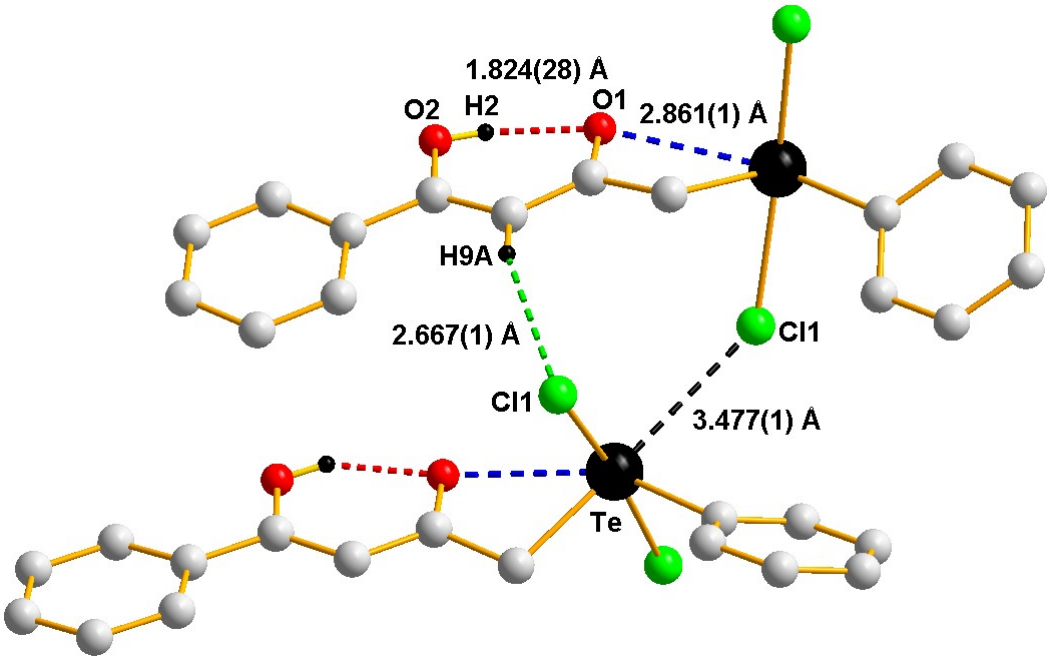

Fig. S2 Crystal lattices of compound **1** showing O-H---O (red), C-H---Cl and (green) hydrogen bonding interactions and Te---O (blue) & Te---Cl (black) secondary bonding interaction.

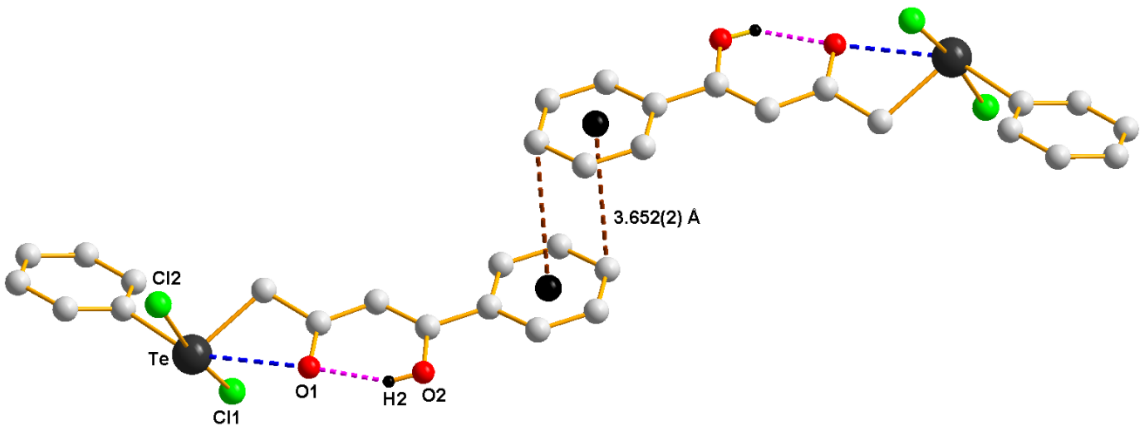

Fig. S3 Crystal lattices of compound **1** showing π---π (brown) interaction.

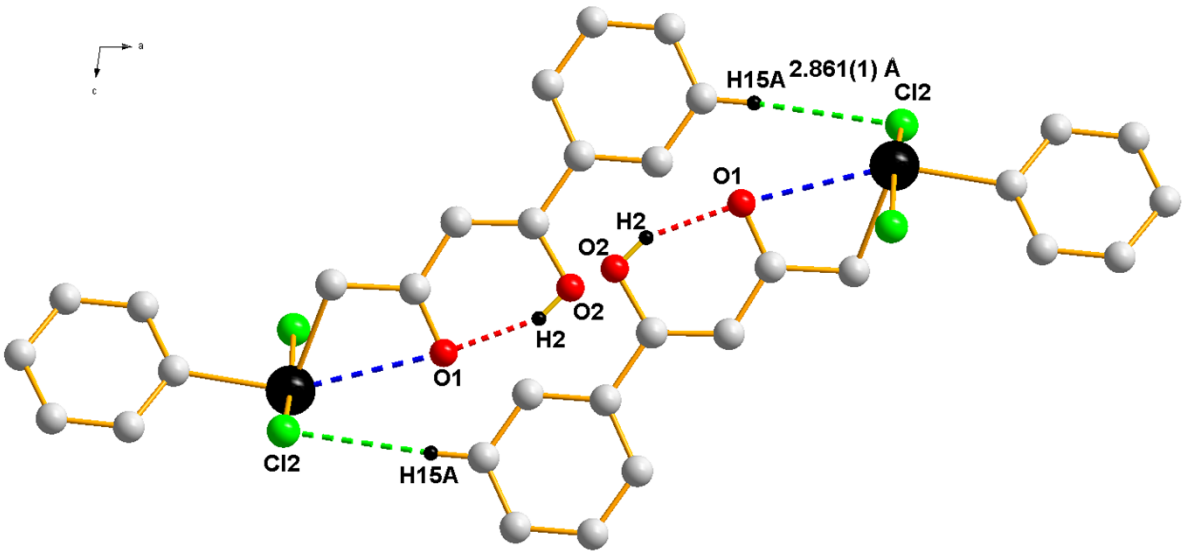

Fig. S4. Centrosymmetric dimeric unit in the crystal lattices of compound **1** through C-H---Cl (green) hydrogen bonding interactions.

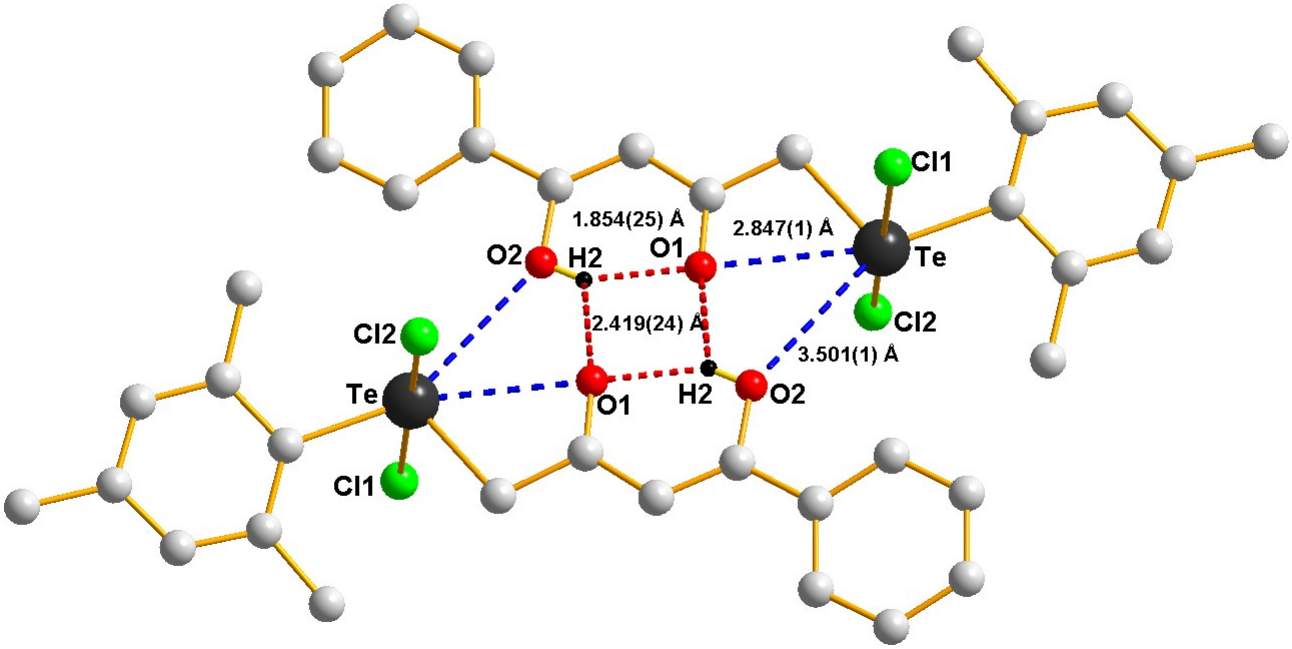

Fig. S5. Centrosymmetric dimeric unit in the crystal lattices of compound **4** through O-H---O (purple) hydrogen bonding interactions, Te---O (blue) secondary bonding interaction.

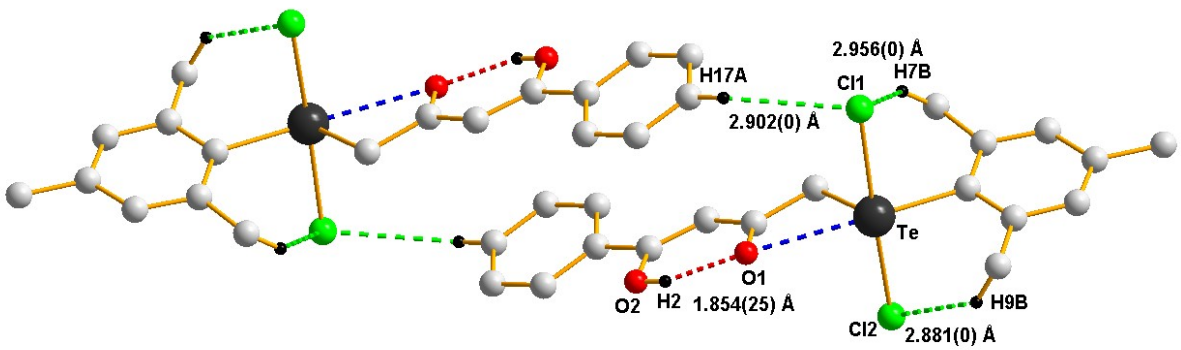

Fig. S6. Centrosymmetric dimeric unit in the crystal lattices of compound **4** through C-H---Cl (green) hydrogen bonding interactions.

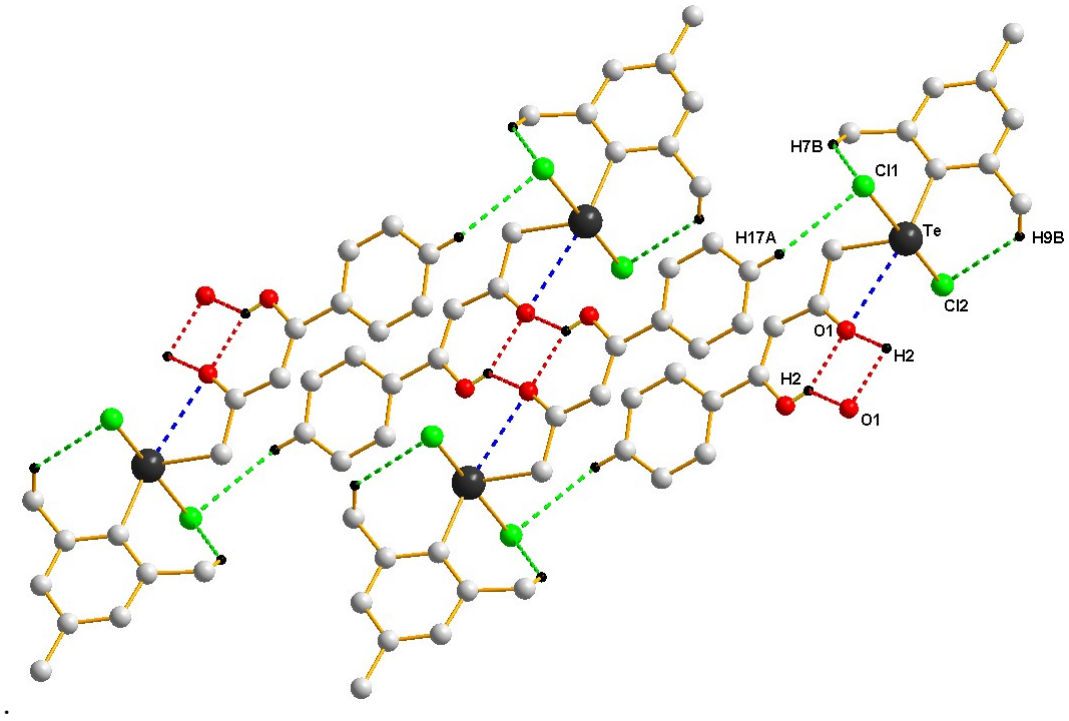

Fig. S7. Supramolecular architecture along c axis of compound **4**.

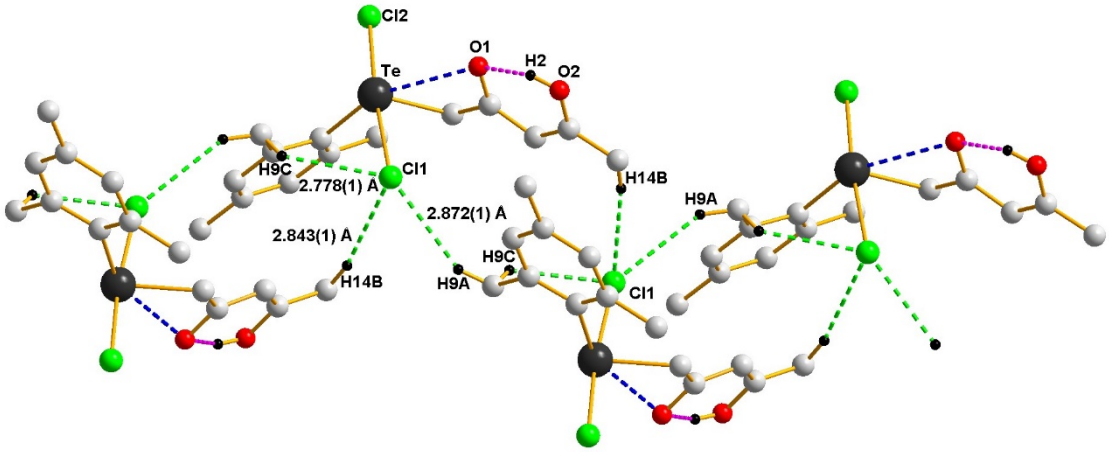

Fig. S8. Supramolecular architectures in the crystal lattices of compound **5** through O-H---O (purple) and C-H---Cl (green) hydrogen bonding interactions and Te---O (blue) secondary bonding interaction.

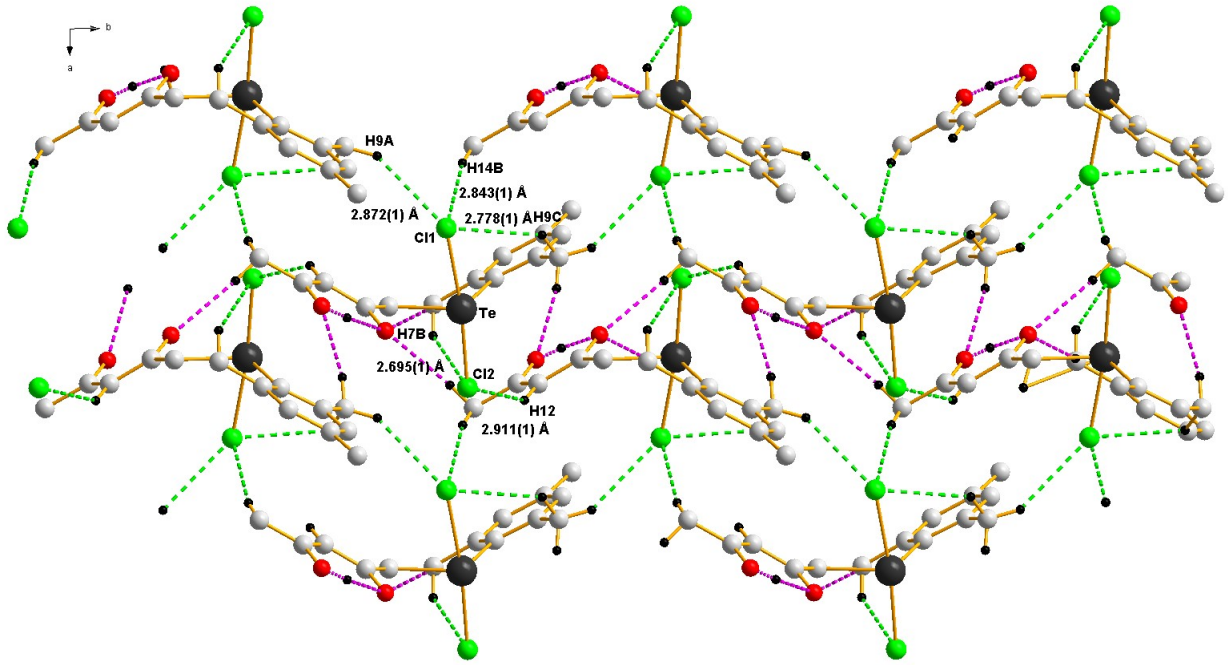

Fig. S9. Supramolecular architectures in the crystal lattices of compound **5** through O-H---O (purple) and C-H---Cl (green) hydrogen bonding interactions.

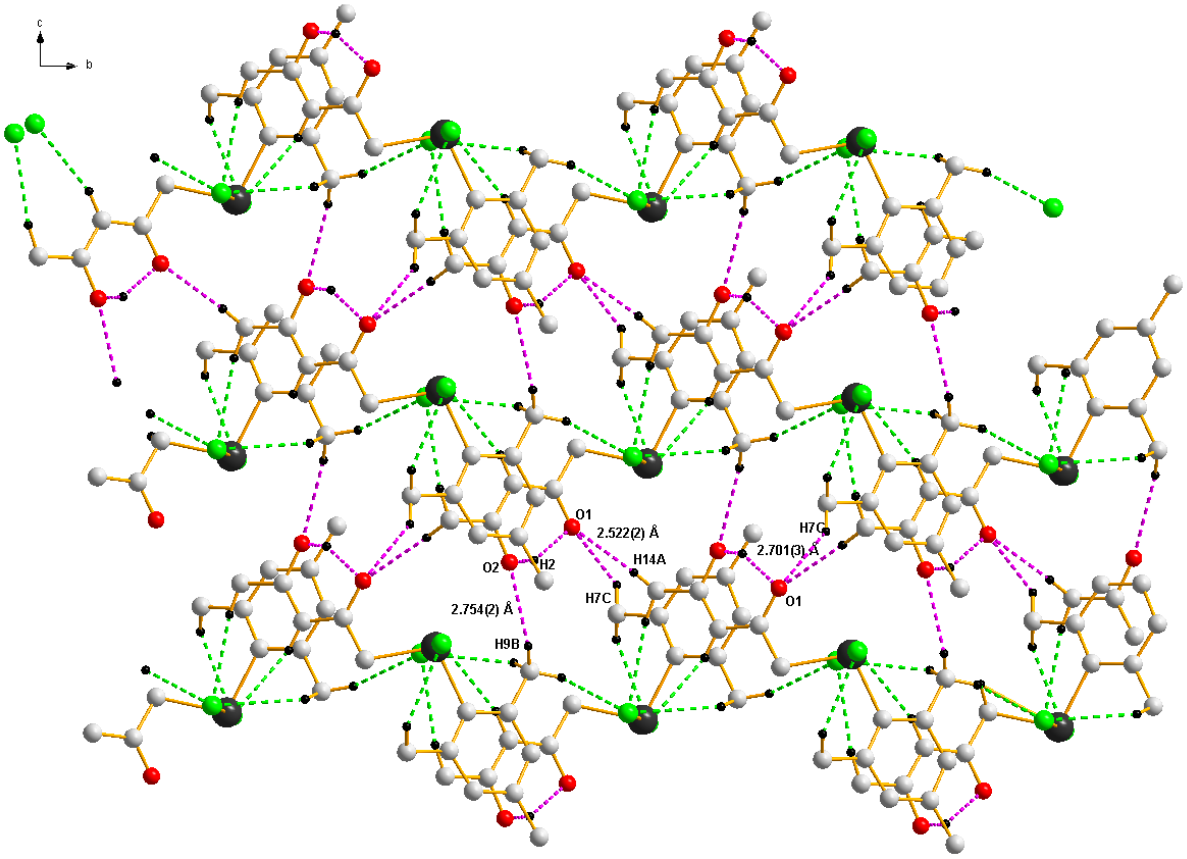

Fig. S10. Supramolecular architectures in the crystal lattices of compound **5** through O-H---O (purple) and C-H---Cl (green) hydrogen bonding interactions.

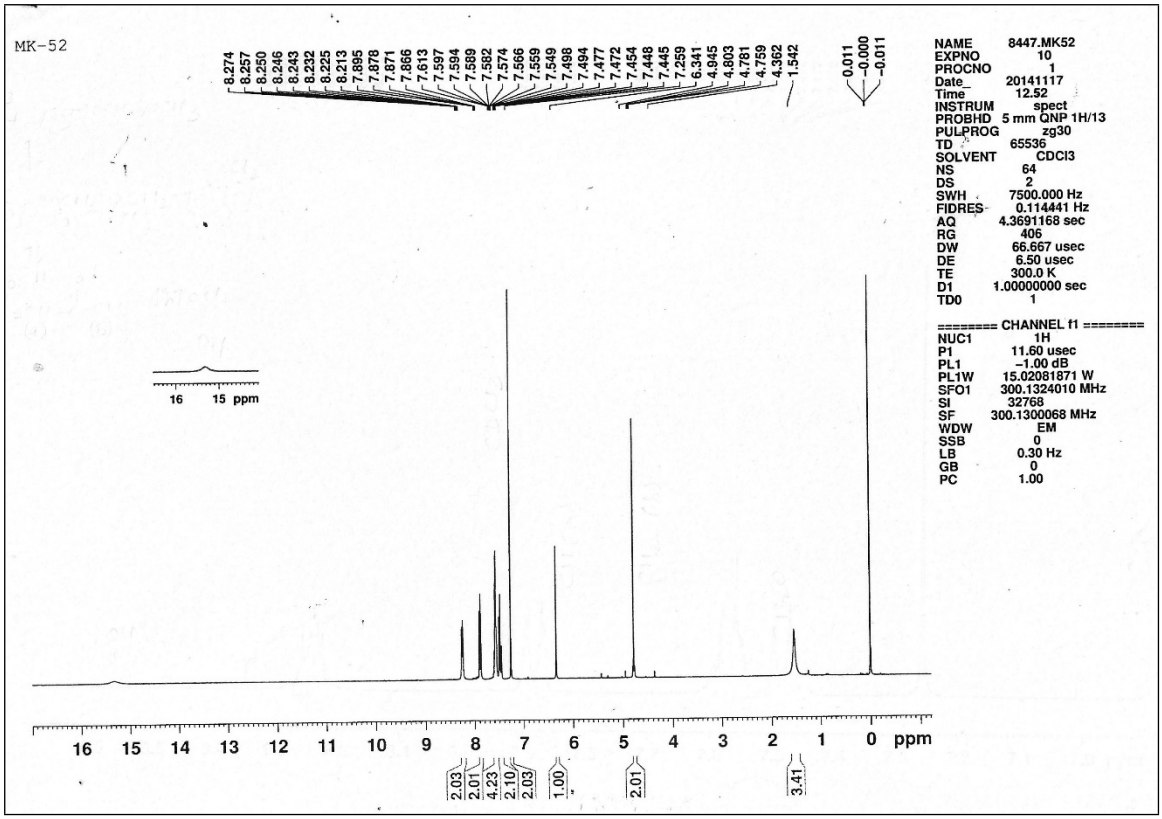

Fig. S11. ^{1}H NMR spectrum of compound Ph[PhC(OH)CHC(O)CH_2]$TeCl_2$ (**1**) in $CDCl_3$.

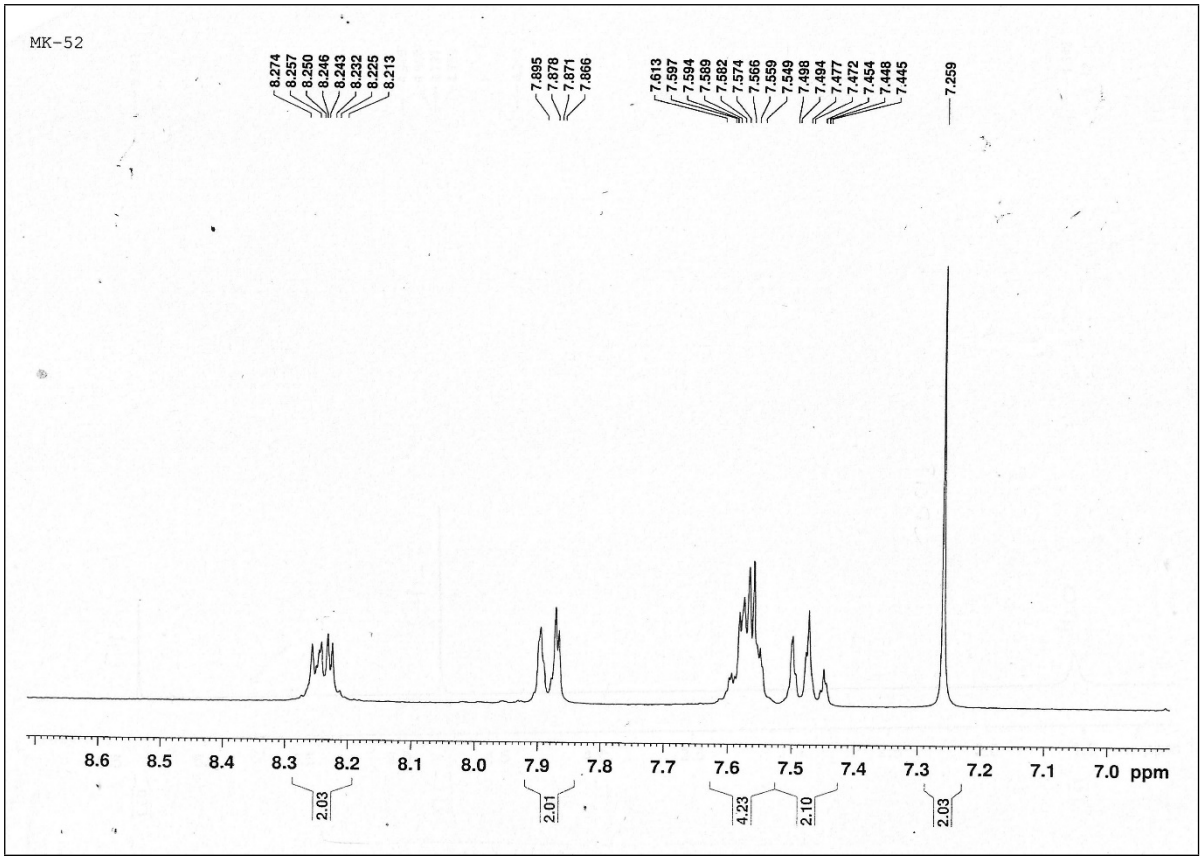

Fig. S12. Expanded aryl region of ^{1}H NMR spectrum of compound $Ph[PhC(OH)CHC(O)CH_2]TeCl_2$ (**1**) in $CDCl_3$.

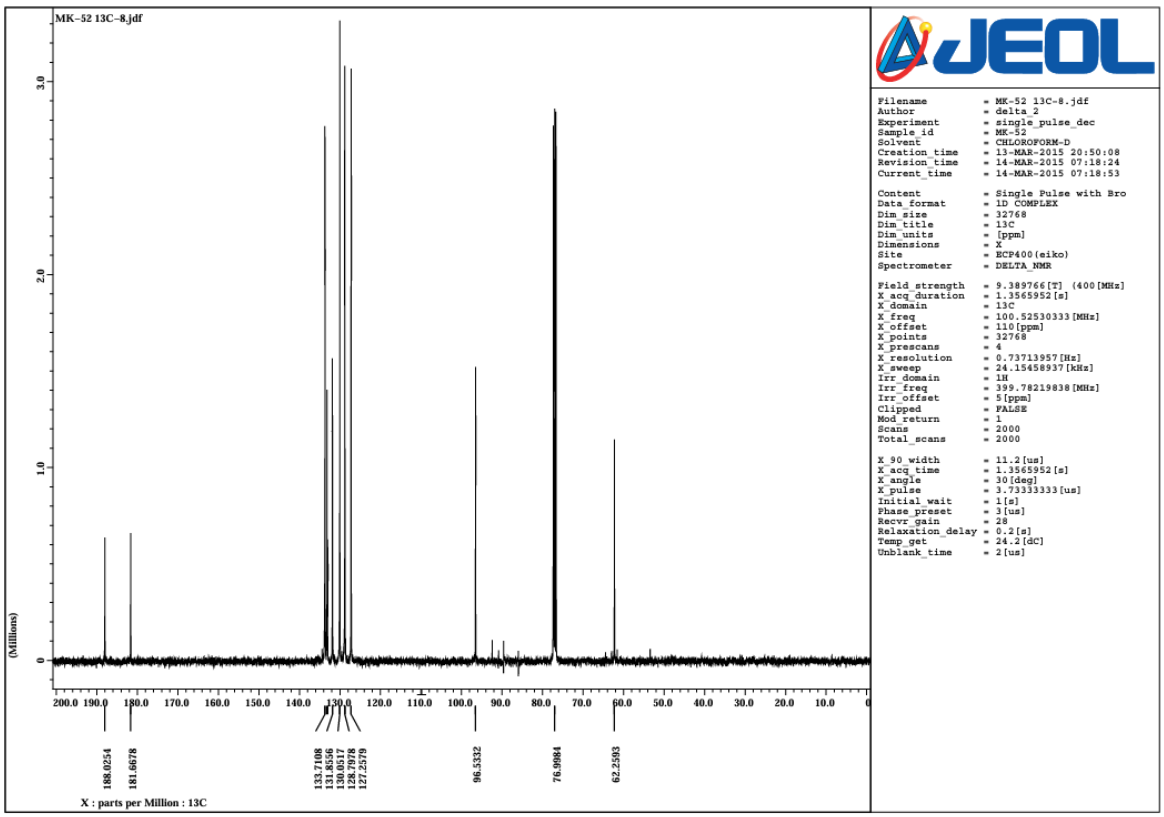

Fig. S13. ^{13}C NMR spectrum of compound Ph[PhC(OH)CHC(O)CH_2]$TeCl_2$ (**1**) in $CDCl_3$.

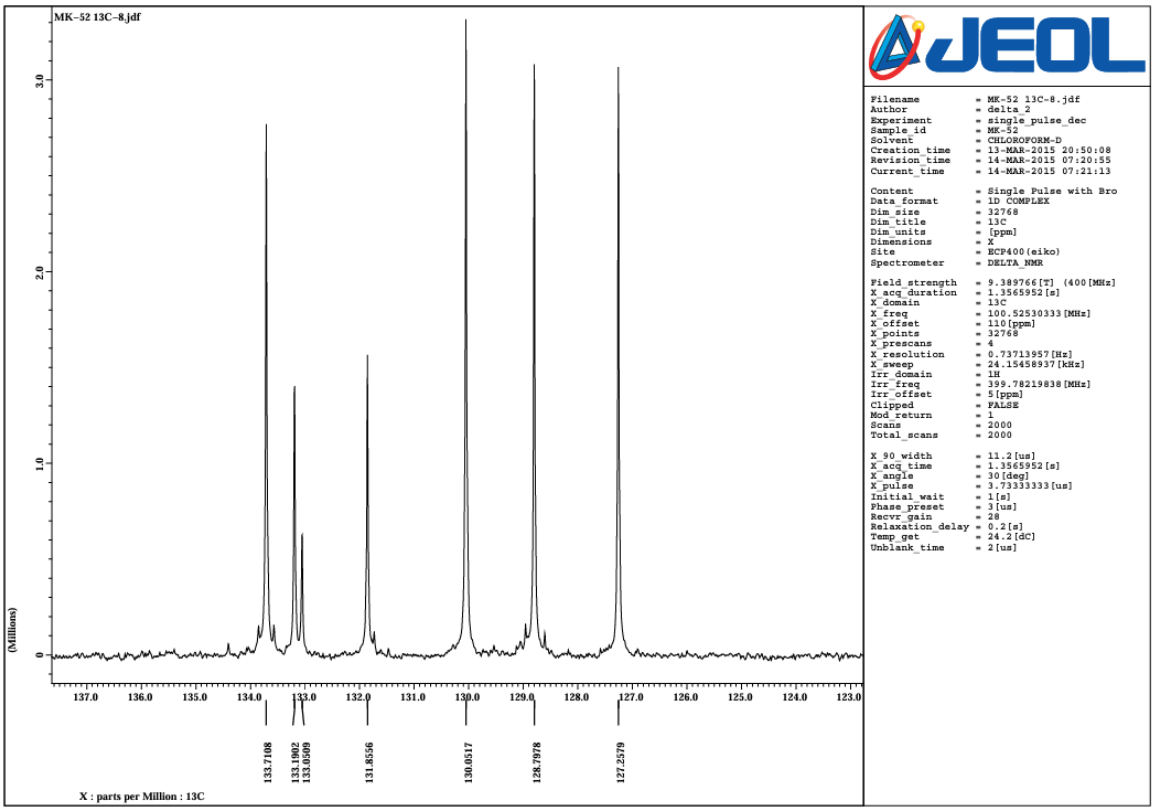

Fig. S14. Expanded aryl region of ^{13}C NMR spectrum of compound $Ph[PhC(OH)CHC(O)CH_2]TeCl_2$ (**1**) in $CDCl_3$.

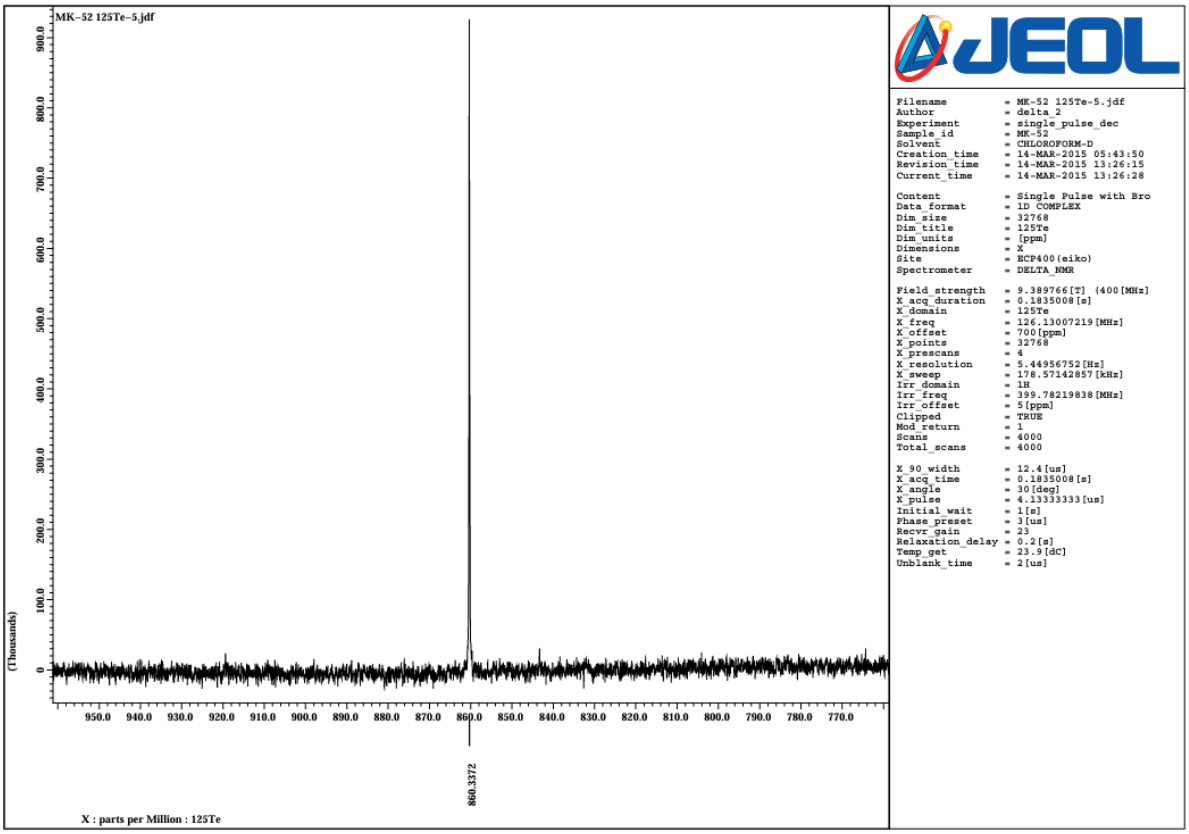

Fig. S15. ^{125}Te NMR spectrum of compound Ph[PhC(OH)CHC(O)CH$_2$]TeCl$_2$ (**1**) in CDCl$_3$.

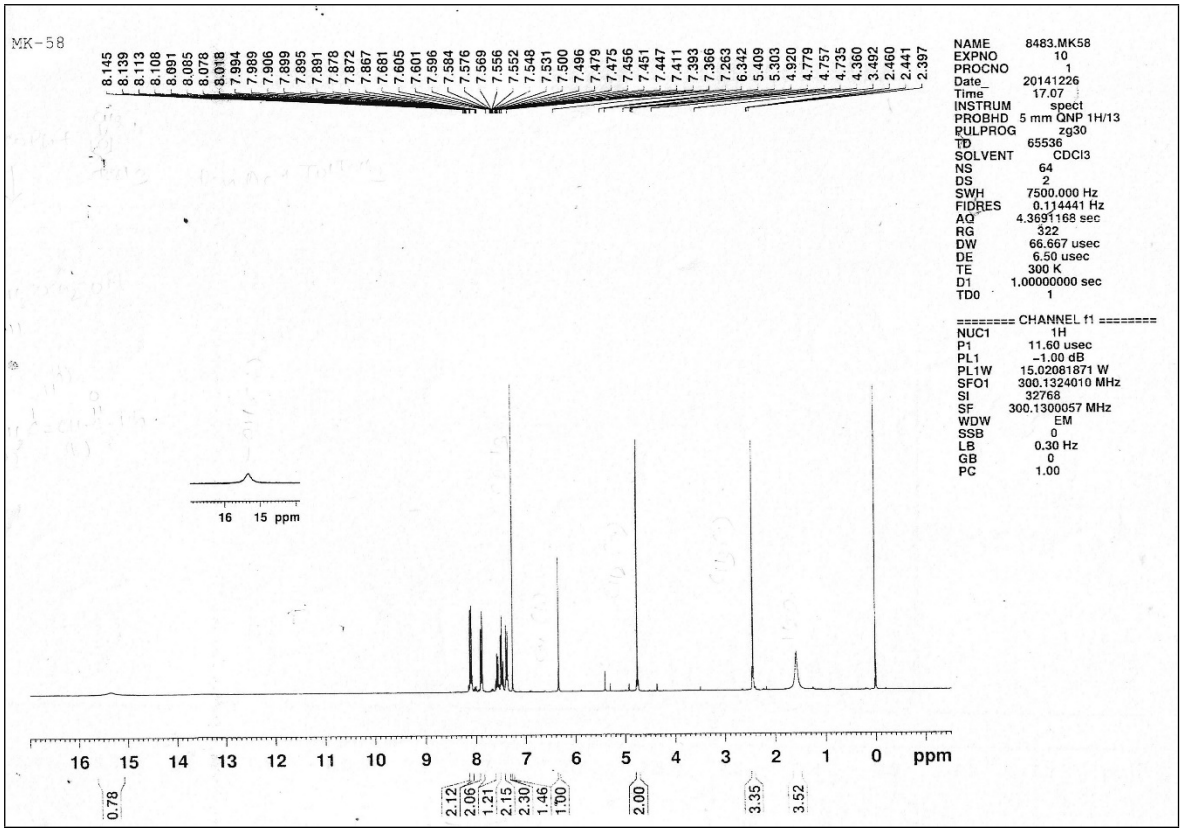

Fig. S16. ^{1}H NMR spectrum of compound *p*-Tol[PhC(OH)CHC(O)CH_2]$TeCl_2$ (**2**) in $CDCl_3$.

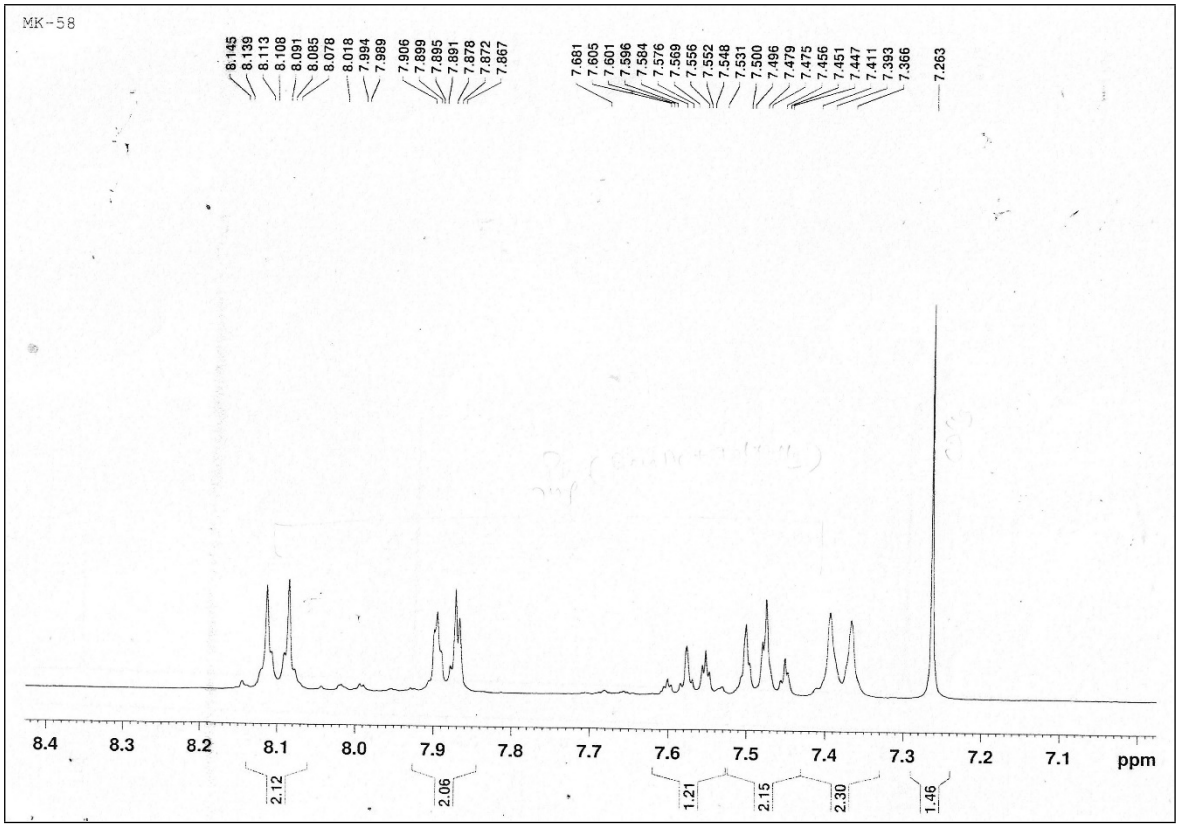

Fig. S17. Expanded aryl region of ^{1}H NMR spectrum of compound *p*-Tol[PhC(OH)CHC(O)CH_2]$TeCl_2$ (**2**) in $CDCl_3$.

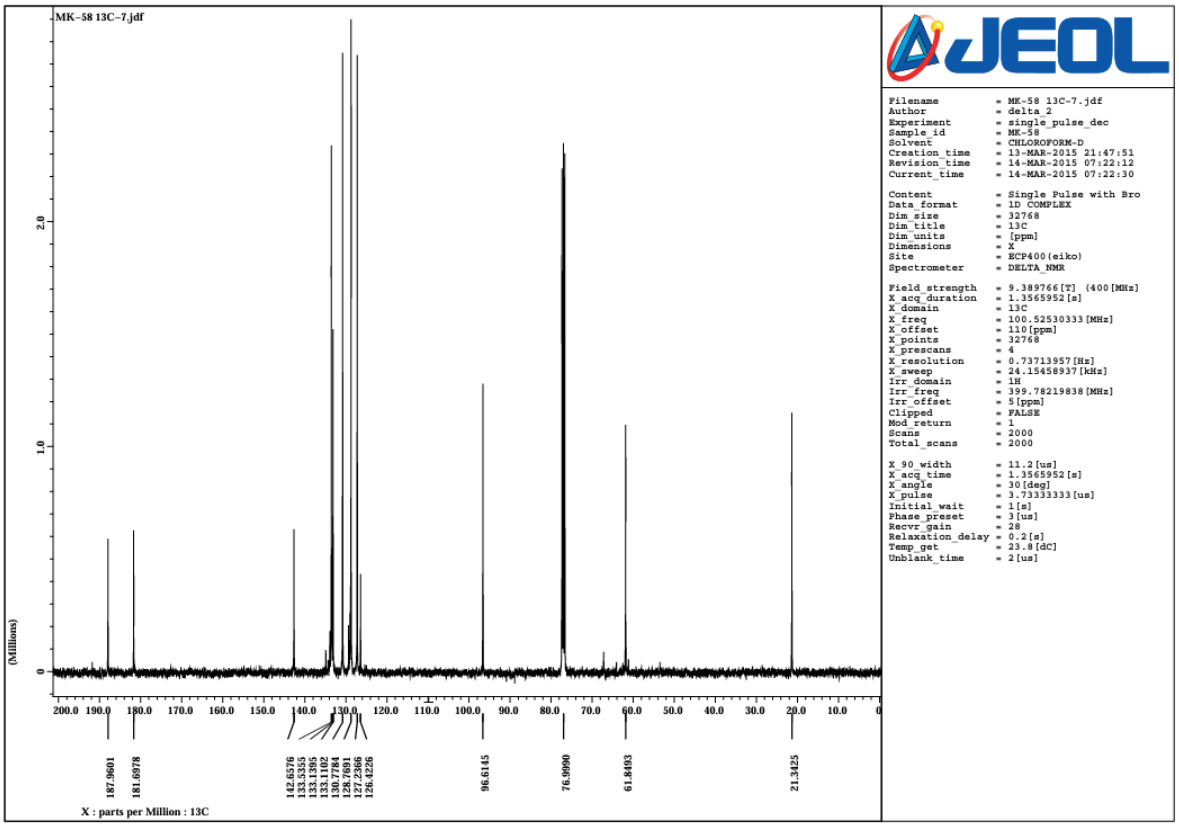

Fig. S18. ^{13}C NMR spectrum of compound *p*-Tol[PhC(OH)CHC(O)CH_2]$TeCl_2$ (**2**) in $CDCl_3$.

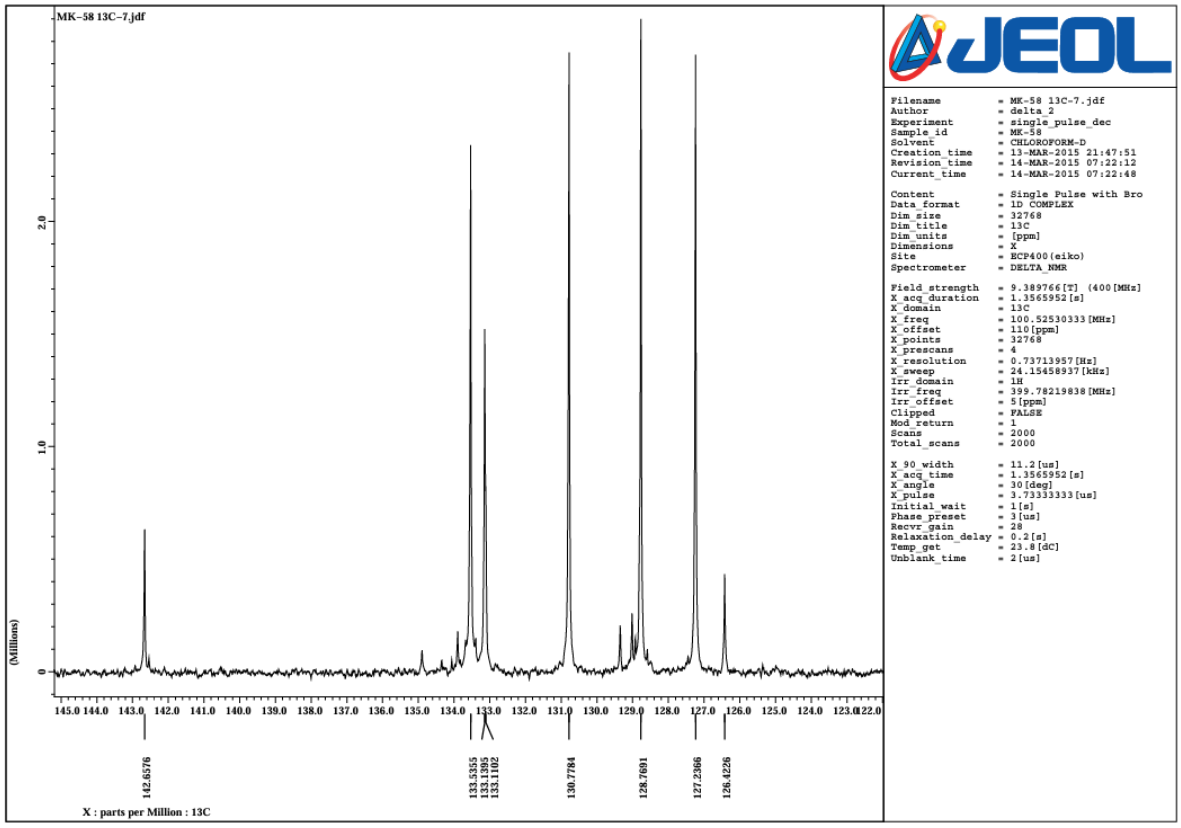

Fig. S19. Expanded aryl region of ^{13}C NMR spectrum of compound *p*-Tol[PhC(OH)CHC(O)CH_2]$TeCl_2$ (**2**) in $CDCl_3$.

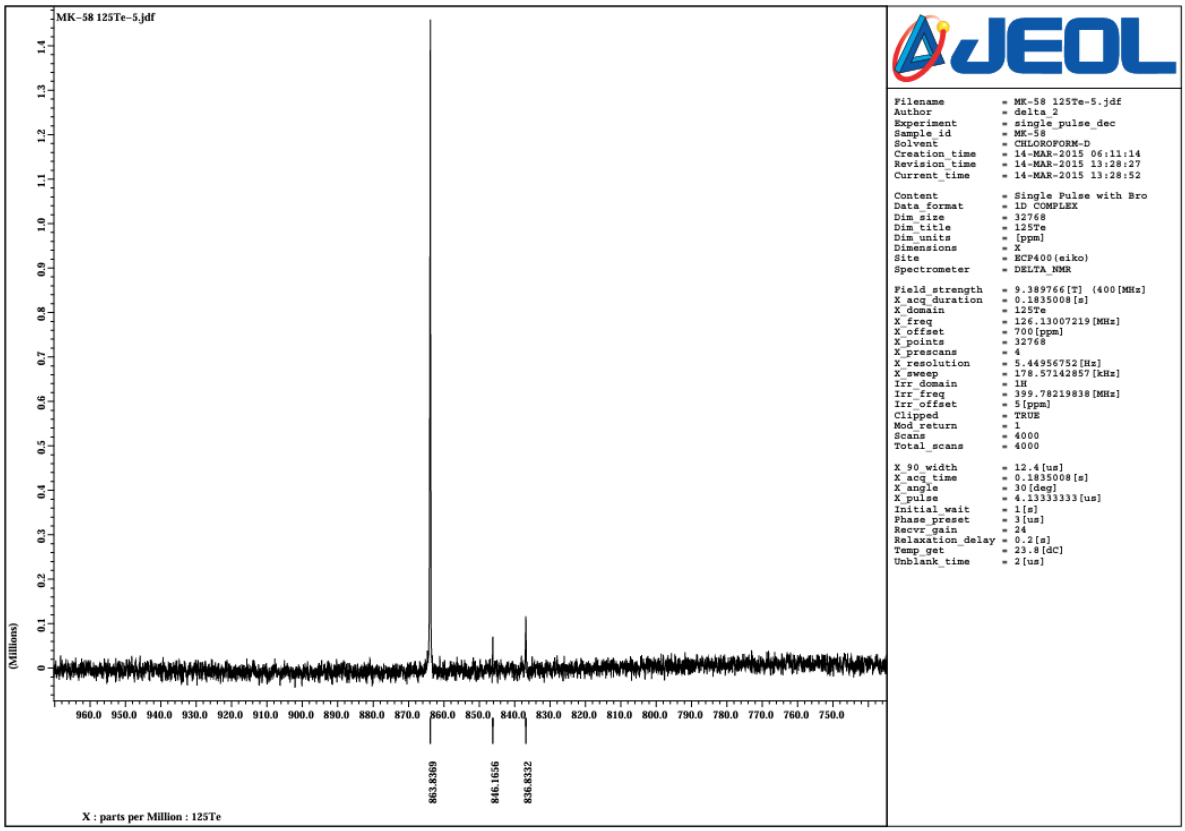

Fig. S20. ^{125}Te NMR spectrum of compound *p*-Tol[PhC(OH)CHC(O)CH_2]$TeCl_2$ (**2**) in $CDCl_3$.

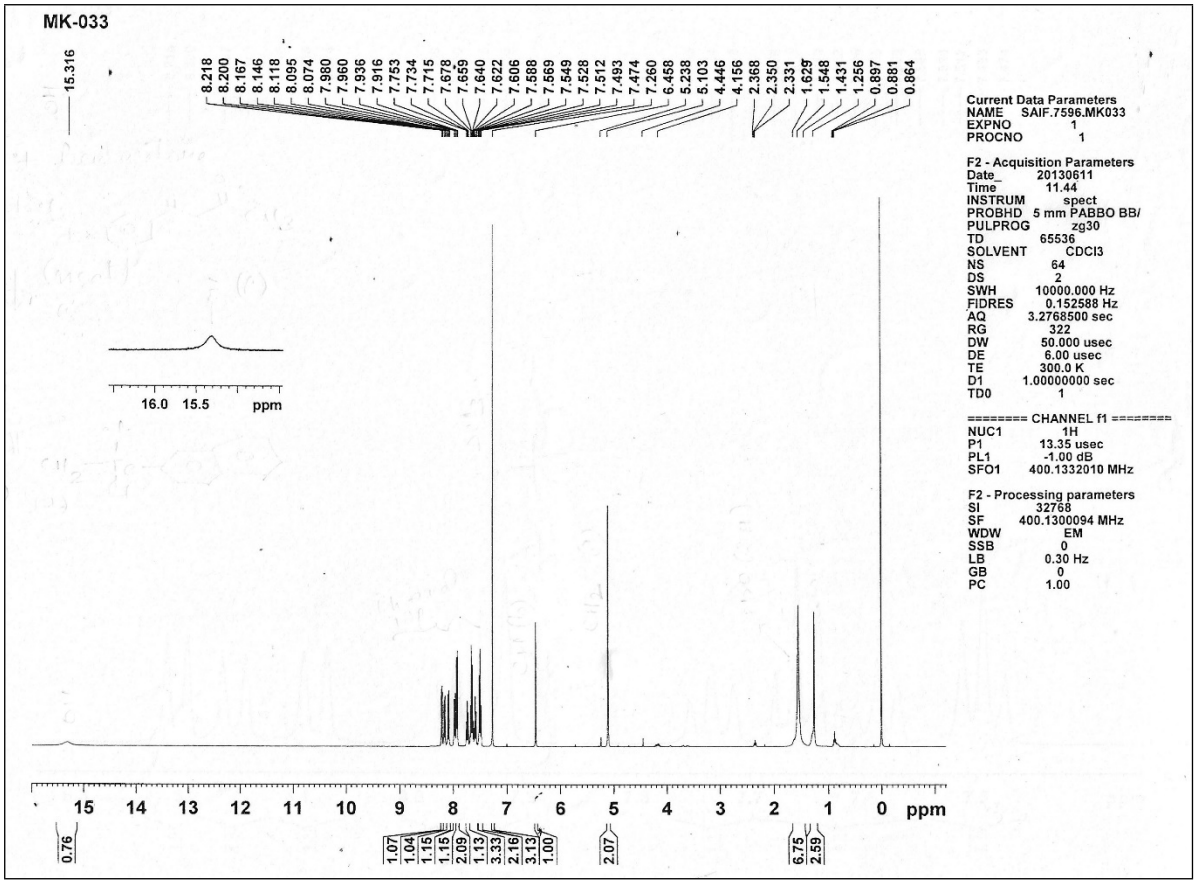

Fig. S21. ^{1}H NMR spectrum of compound *1*-Nap[PhC(OH)CHC(O)CH_2]$TeCl_2$ (**3**) in $CDCl_3$.

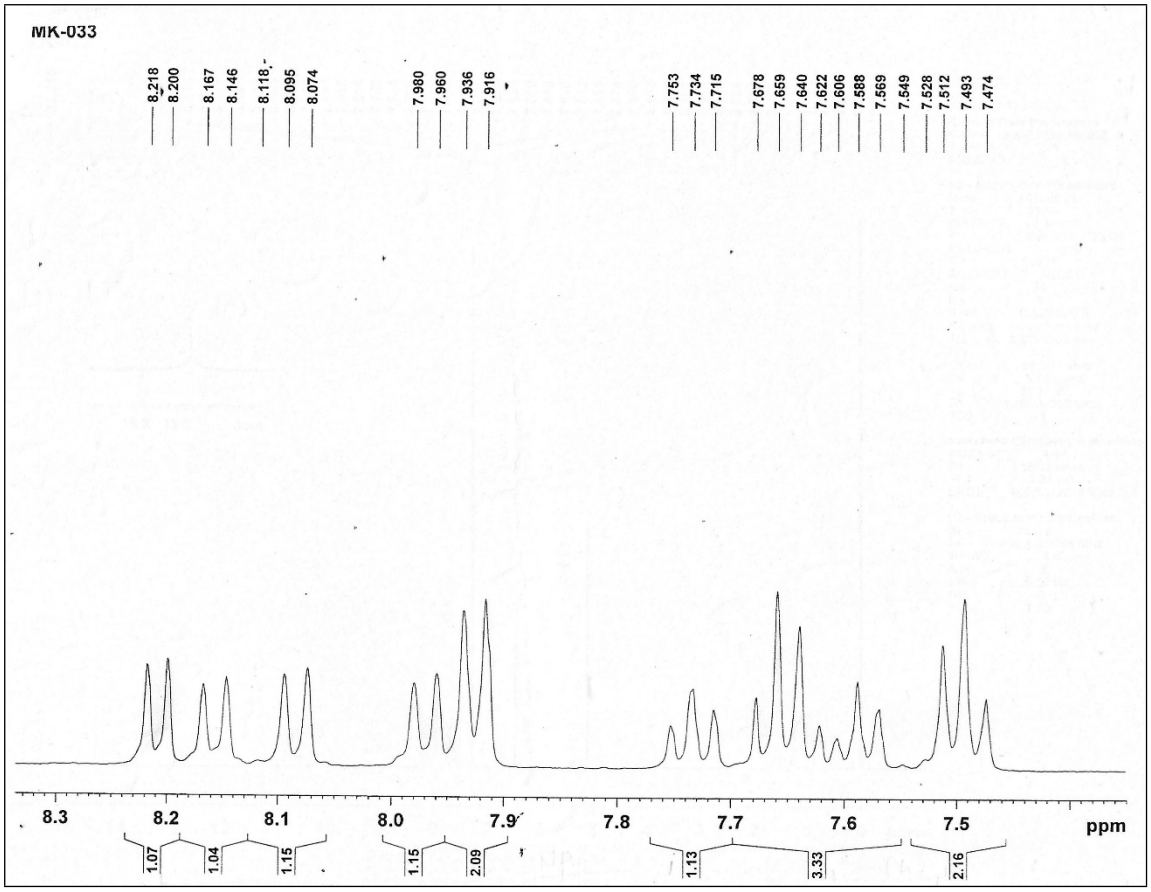

Fig. S22. Expanded aryl region of ^{1}H NMR spectrum of compound *1*-Nap[PhC(OH)CHC(O)CH_2]$TeCl_2$ (**3**) in $CDCl_3$.

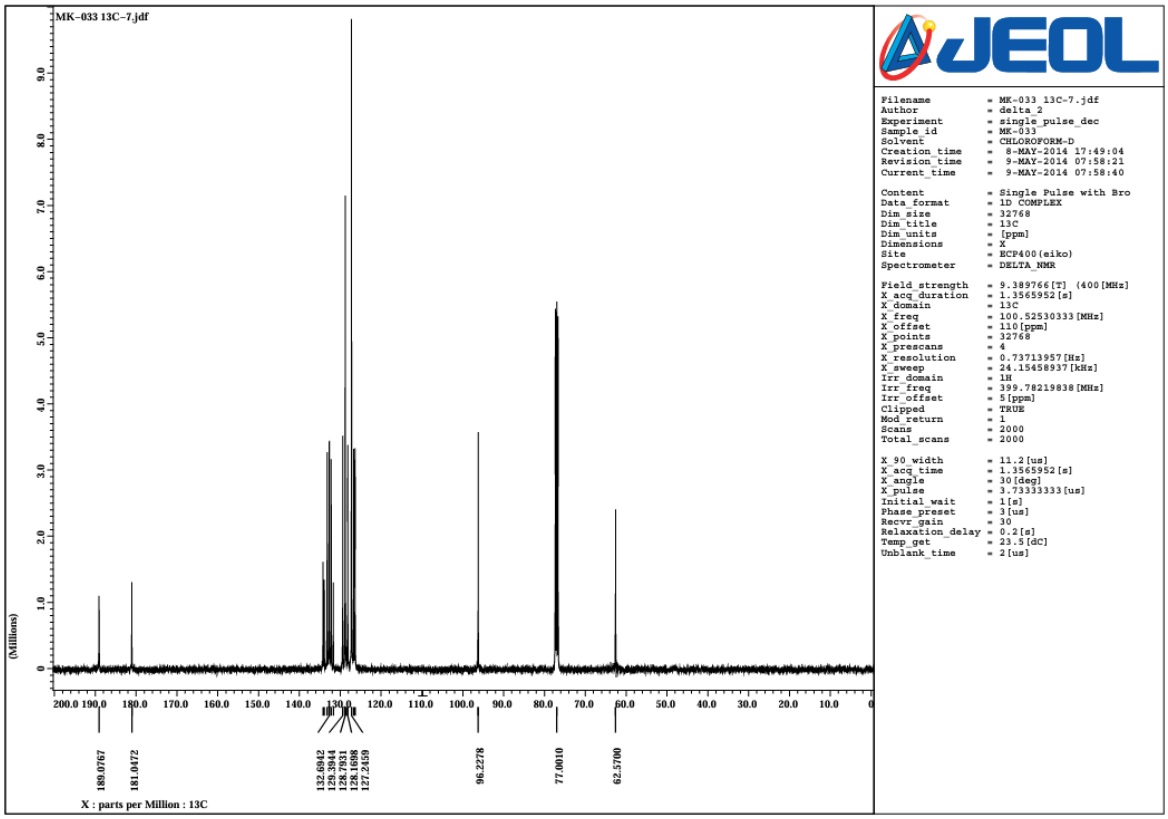

Fig. S23. ^{13}C NMR spectrum of compound *1*-Nap[PhC(OH)CHC(O)CH_2]$TeCl_2$ (**3**) in $CDCl_3$.

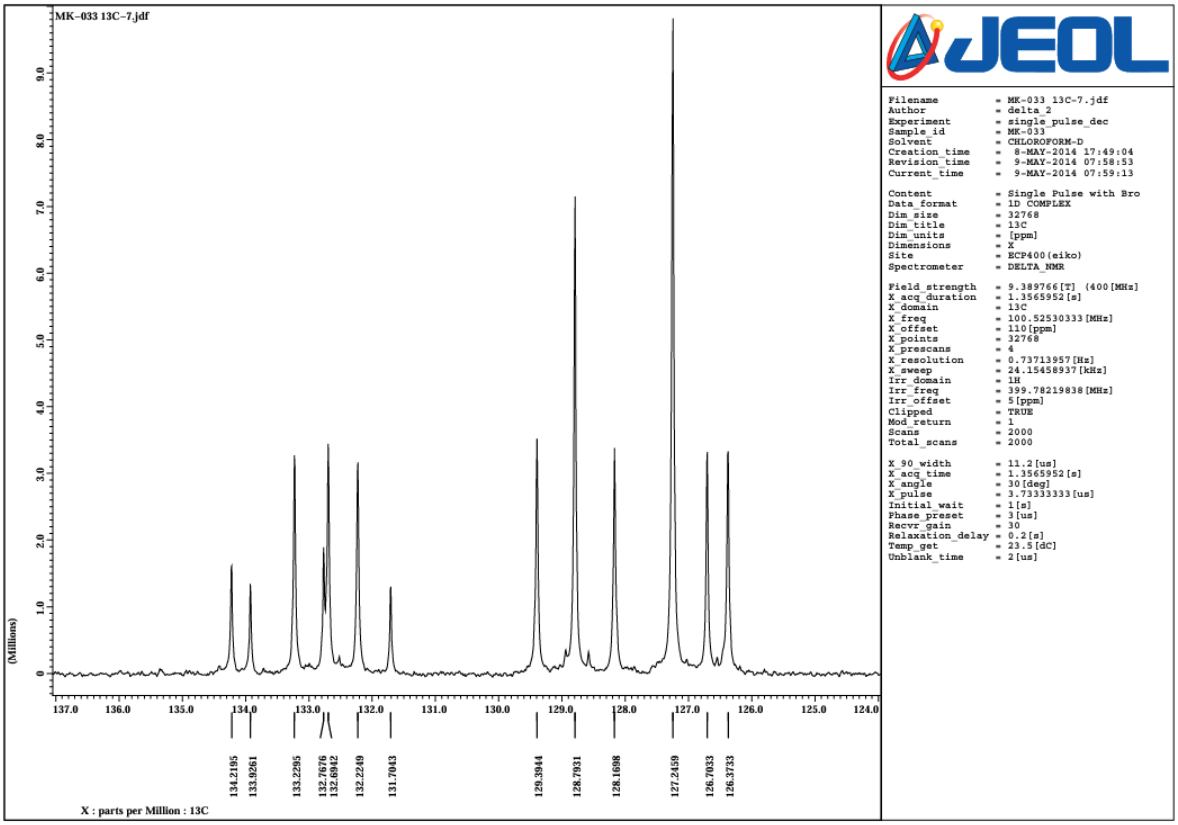

Fig. S24. Expanded aryl region of ^{13}C NMR spectrum of compound *1*-Nap[PhC(OH)CHC(O)CH_2]$TeCl_2$ (**3**) in $CDCl_3$.

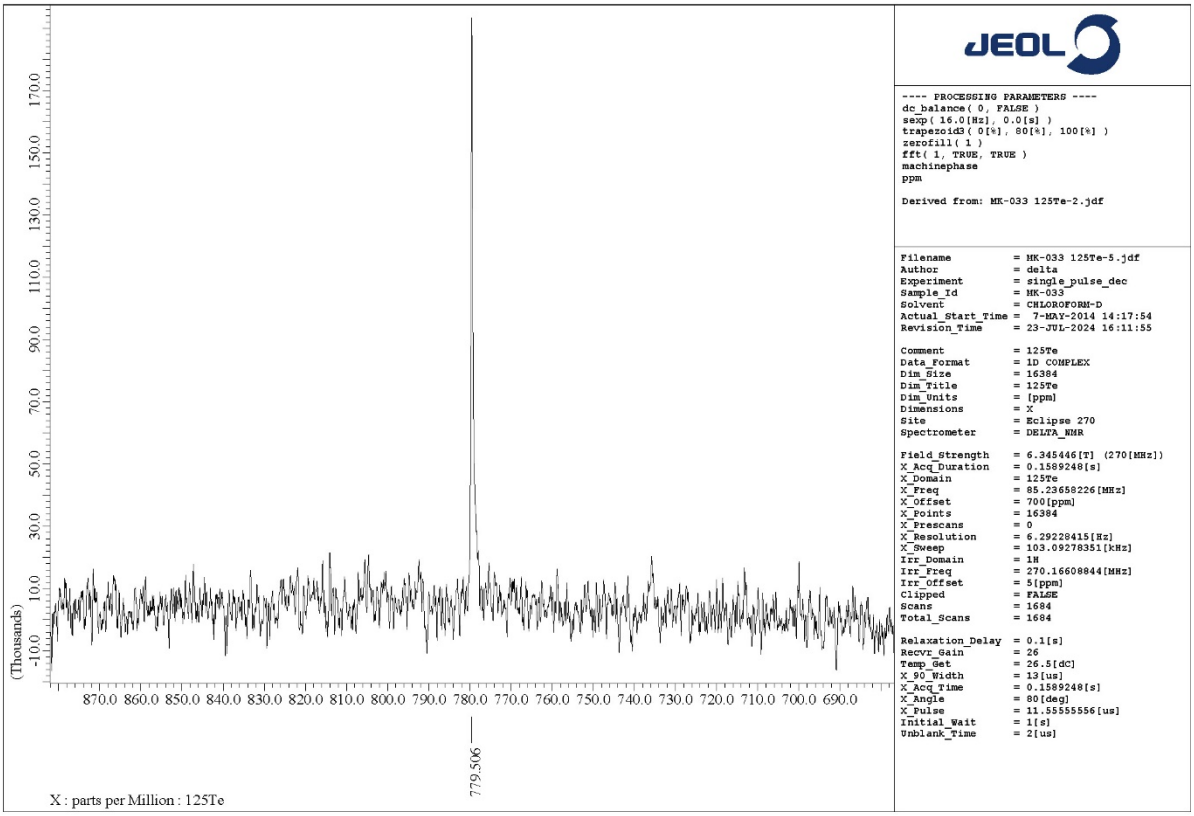

Fig. S25. ^{125}Te NMR spectrum of compound *1*-Nap[PhC(OH)CHC(O)CH_2]$TeCl_2$ (**3**) in $CDCl_3$.

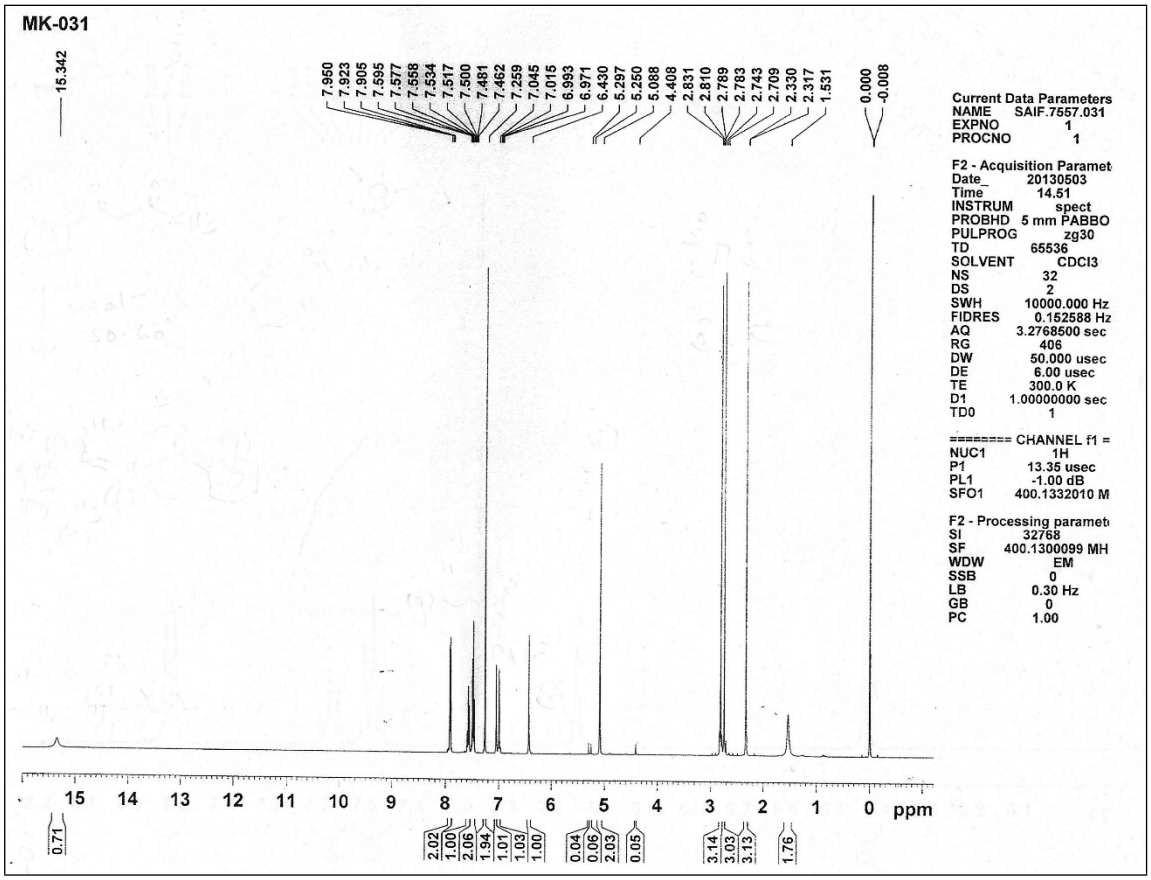

Fig. S26. ^{1}H NMR spectrum of compound Mes[PhC(OH)CHC(O)CH_2]$TeCl_2$ (**4**).

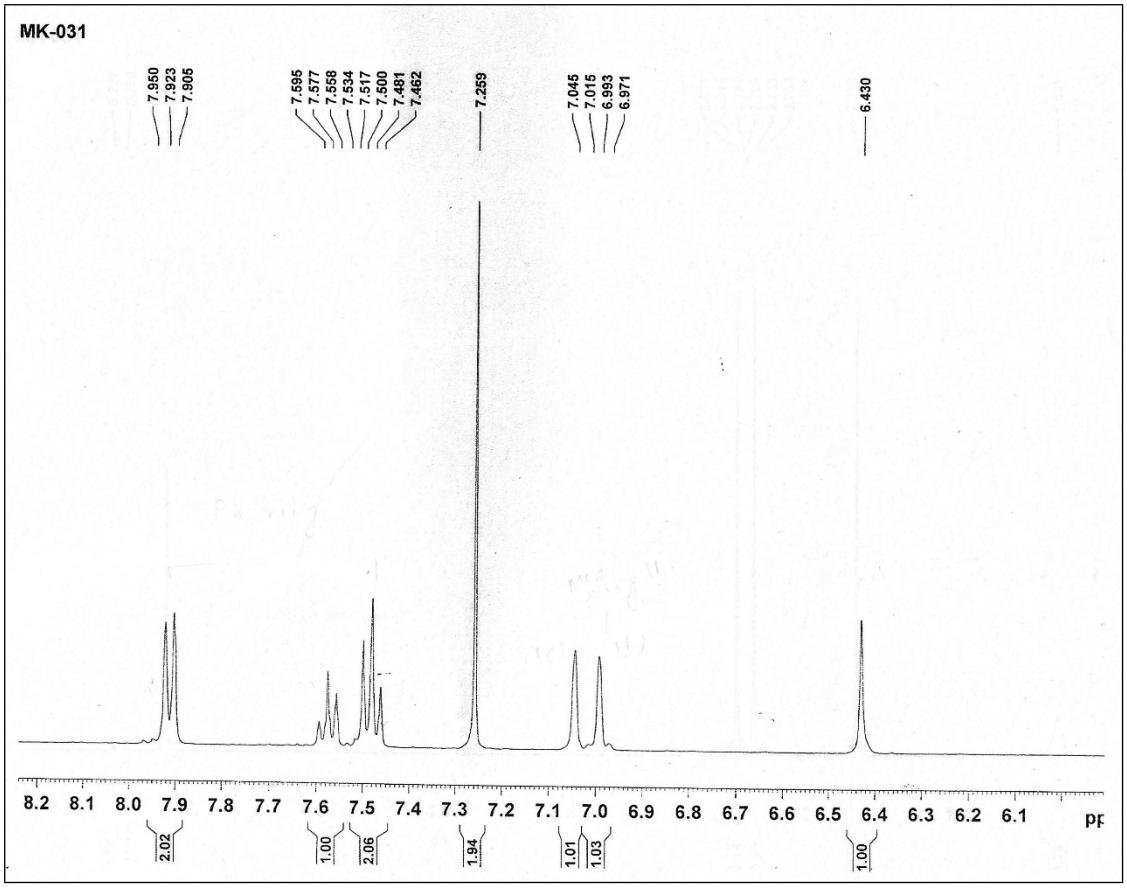

Fig. S27. Expanded aryl region of ^{1}H NMR spectrum of compound Mes[PhC(OH)CHC(O)CH_2]$TeCl_2$ (**4**).

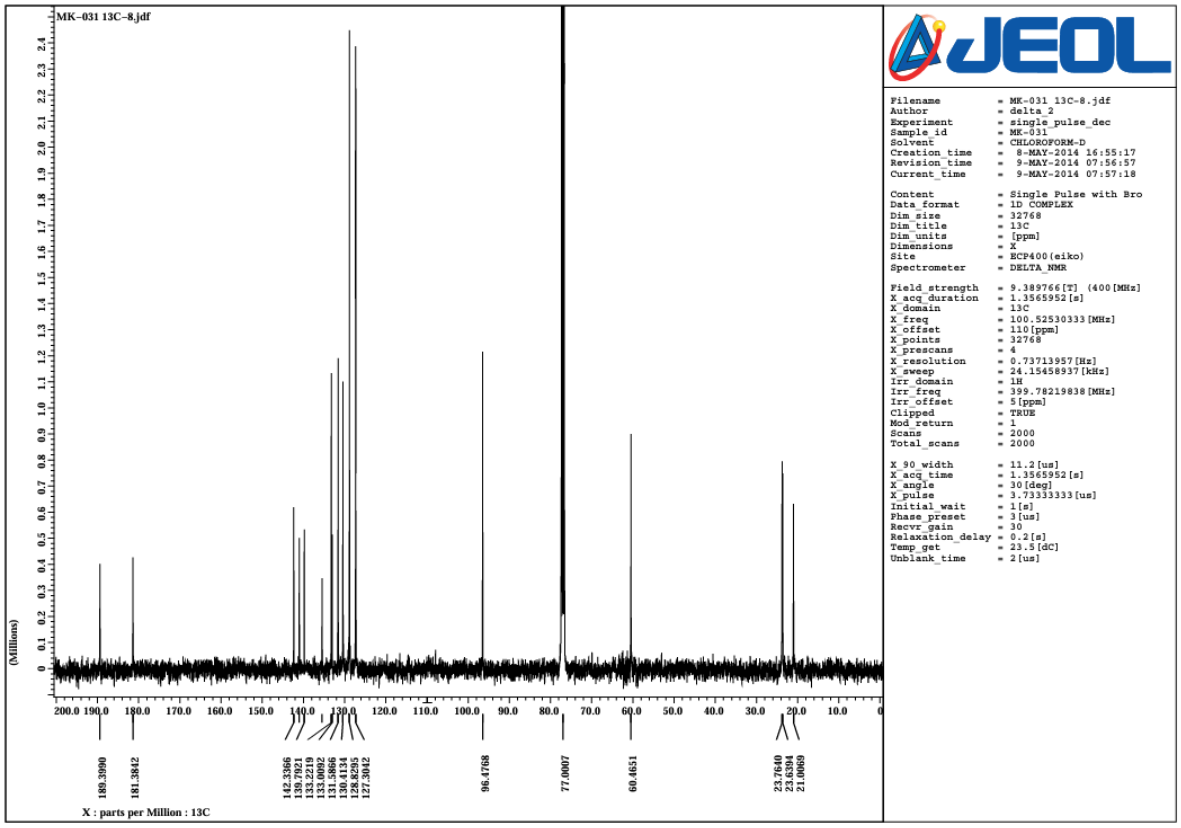

Fig. S28. ^{13}C NMR spectrum of compound Mes[PhC(OH)CHC(O)CH_2]$TeCl_2$ (**4**) in $CDCl_3$.

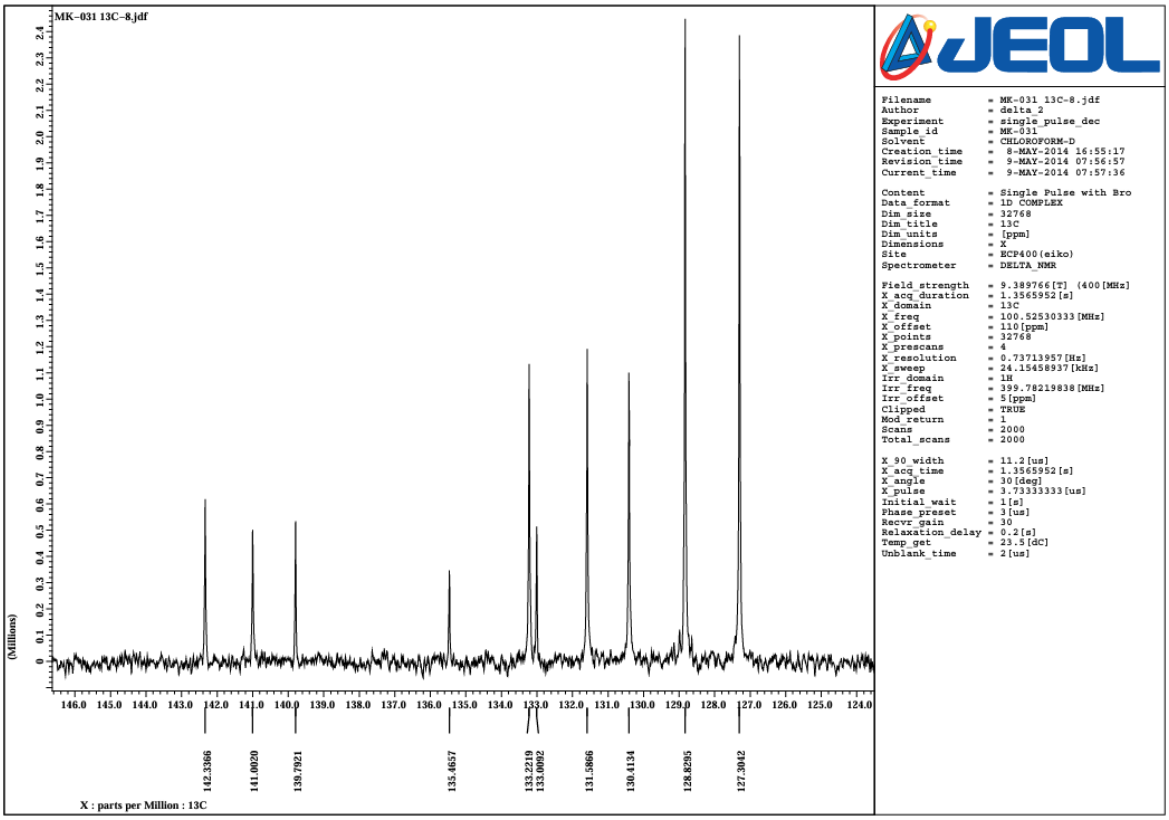

Fig. S29. Expanded aryl region of ^{13}C NMR spectrum of compound Mes[PhC(OH)CHC(O)CH_2]$TeCl_2$ (**4**) in $CDCl_3$.

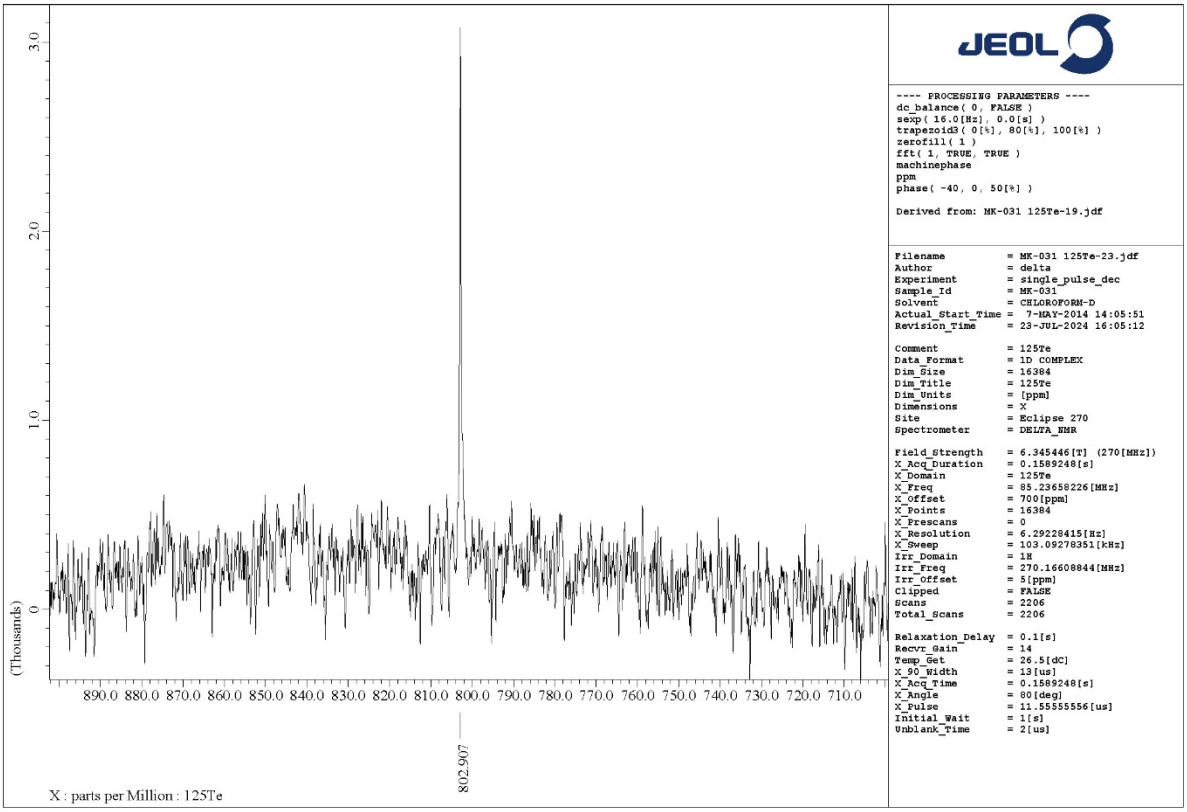

Fig. S30. ^{125}Te NMR spectrum of compound Mes[PhC(OH)CHC(O)CH$_2$]TeCl$_2$ (**4**) in CDCl$_3$.

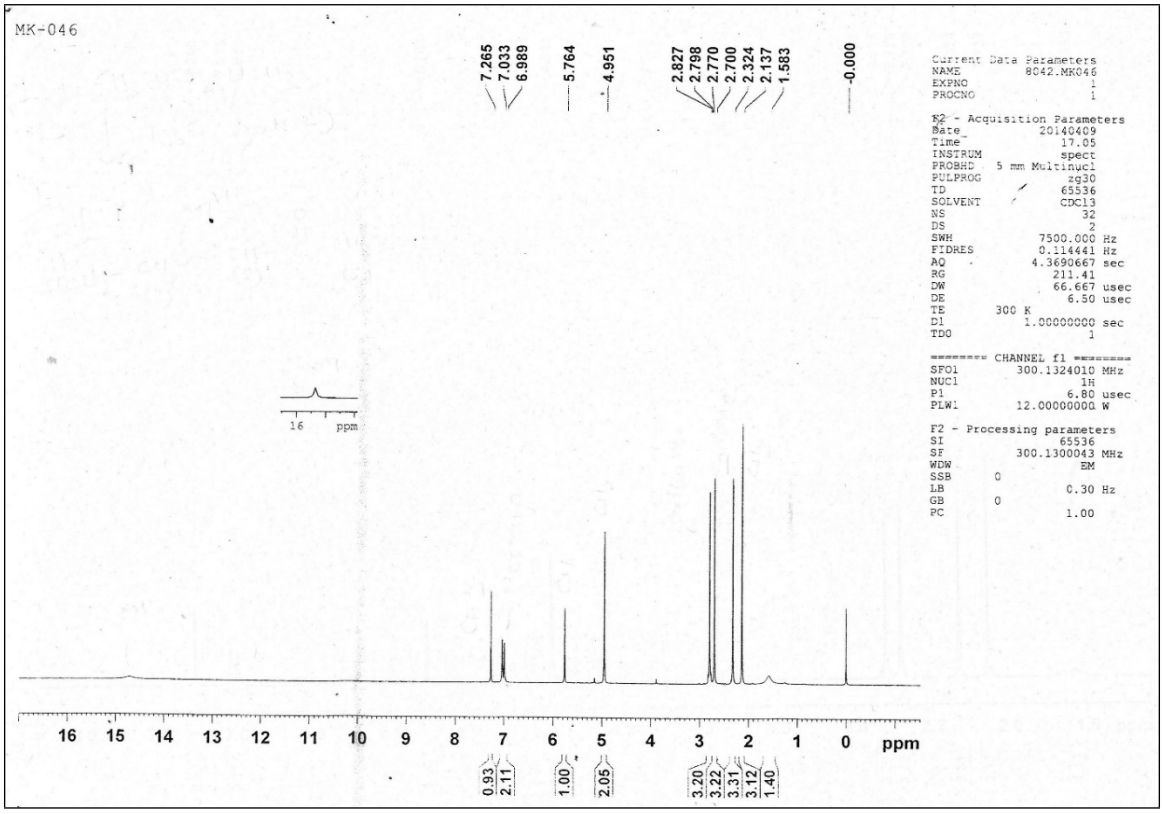

Fig. S31. ^{1}H NMR spectrum of compound Mes[CH_3(OH)CHC(O)CH_2]$TeCl_2$ (**5**).

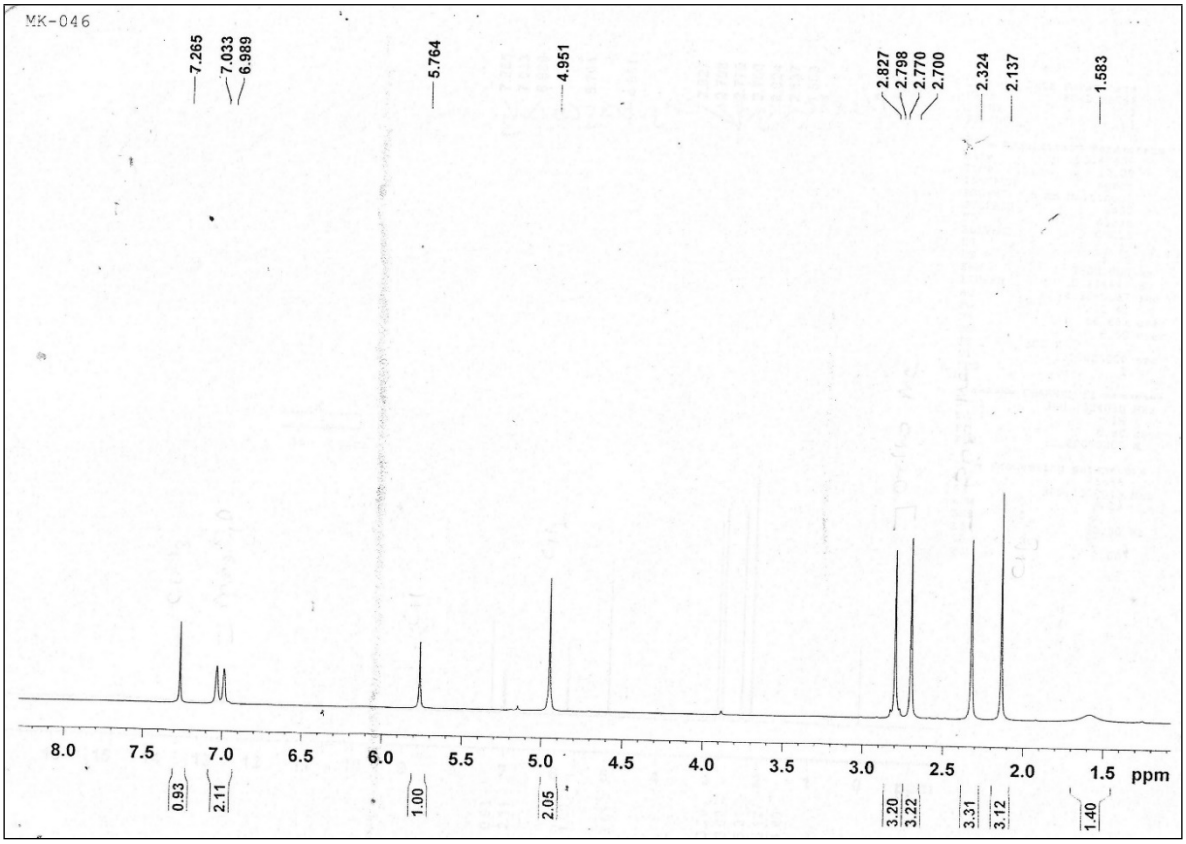

Fig. S32. Expanded aryl region of ^{1}H NMR spectrum of compound $Mes[CH_3(OH)CHC(O)CH_2]TeCl_2$ (**5**).

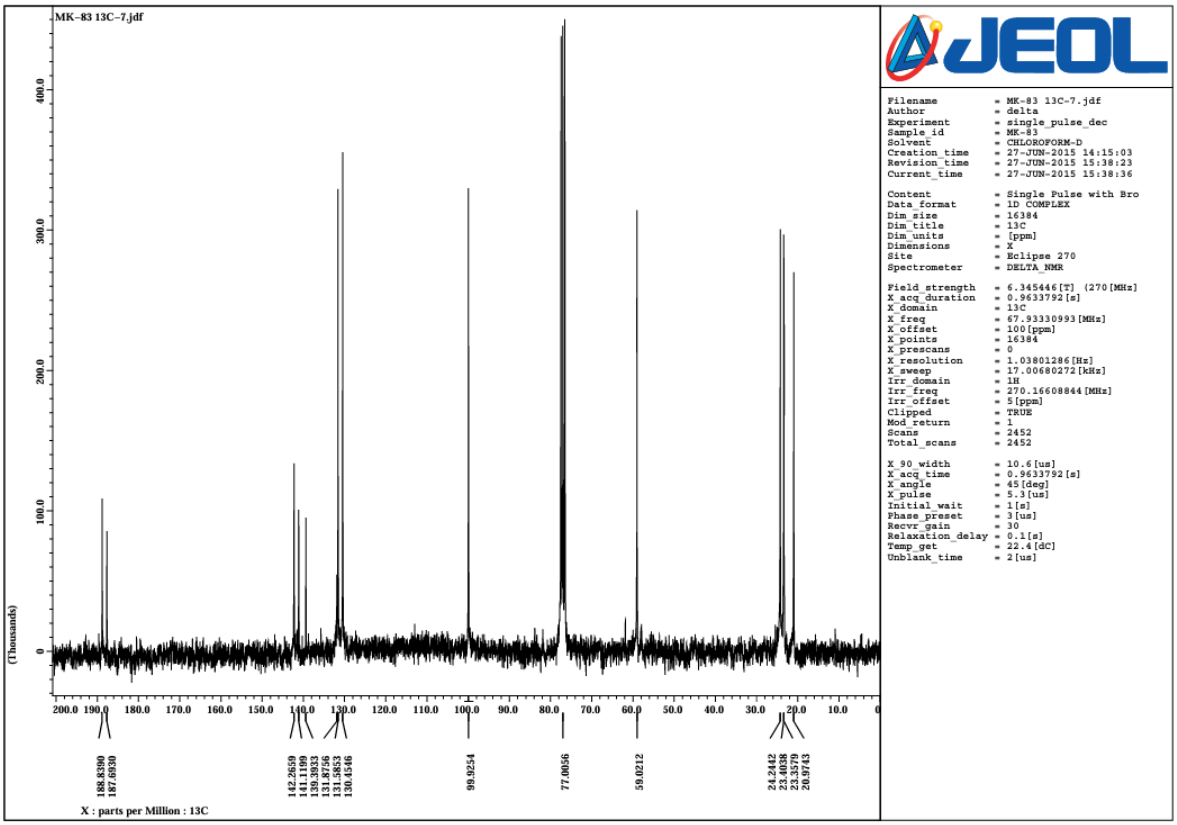

Fig. S33. ^{13}C NMR spectrum of compound Mes[CH_3(OH)CHC(O)CH_2]$TeCl_2$ (**5**) in $CDCl_3$.

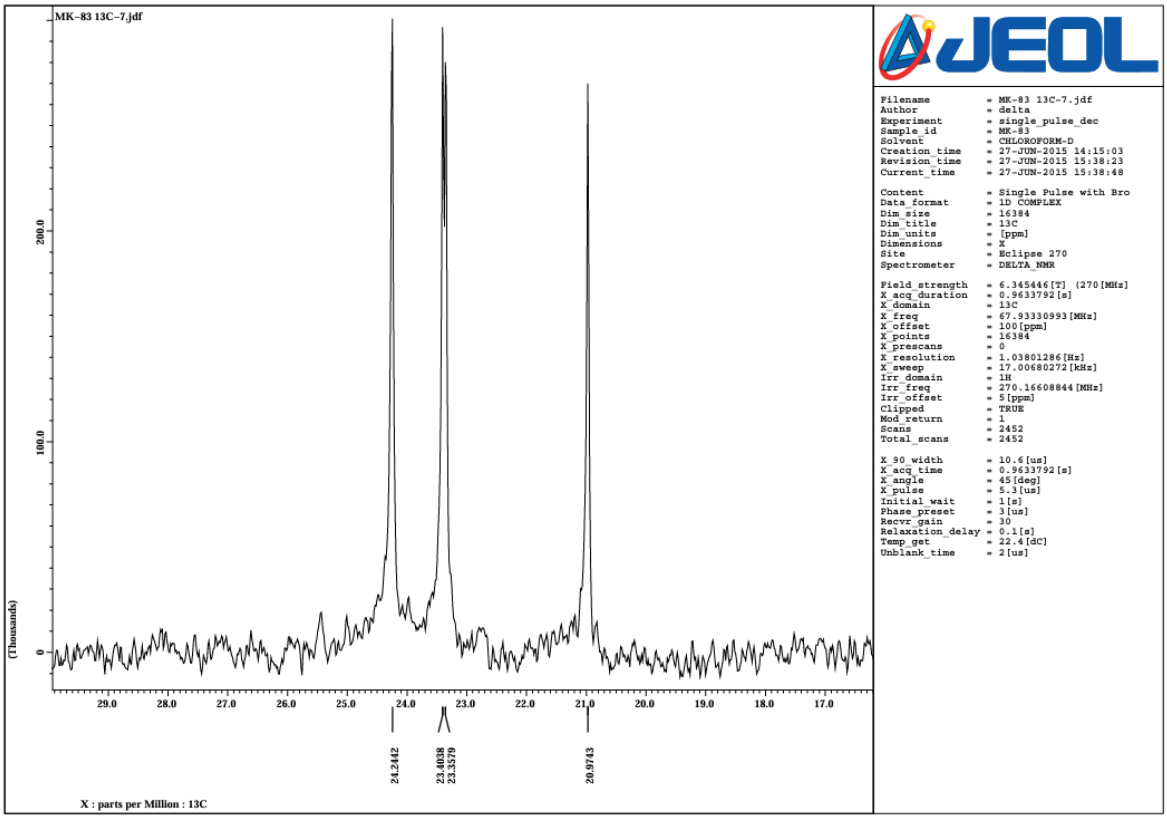

Fig. S34. Expanded alkyl region of ^{13}C NMR spectrum of compound $Mes[CH_3(OH)CHC(O)CH_2]TeCl_2$ (**5**) in $CDCl_3$.

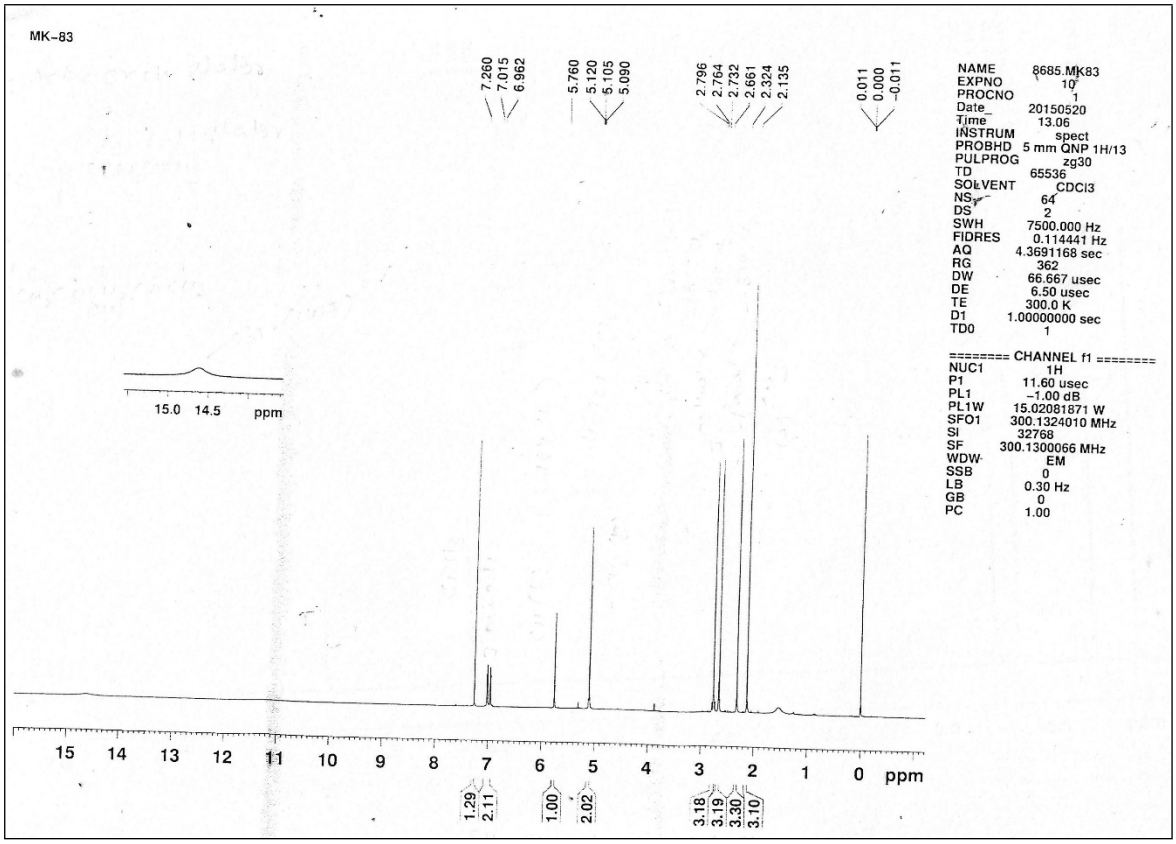

Fig. S35. ^{1}H NMR spectrum of compound Mes[CH_3(OH)CHC(O)CH_2]$TeBr_2$ (**6**).

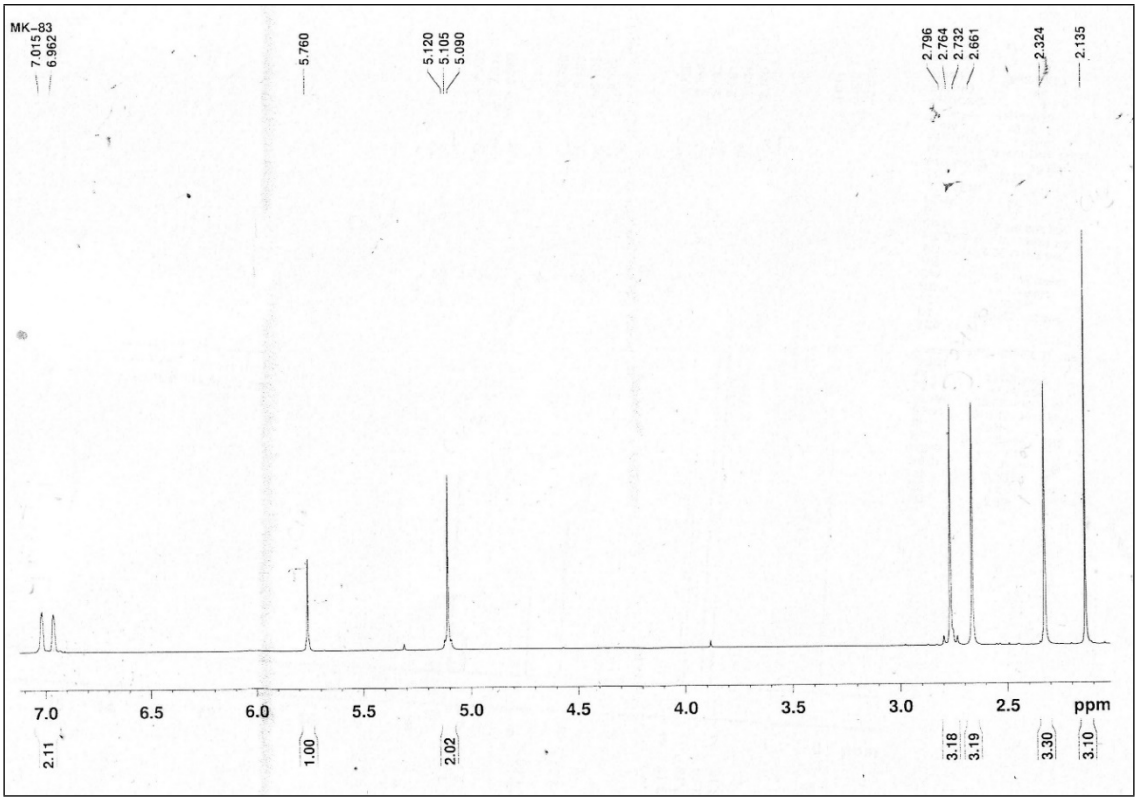

Fig. S36. ^{1}H NMR spectrum of compound Mes[CH_3(OH)CHC(O)CH_2]$TeBr_2$ (**6**).

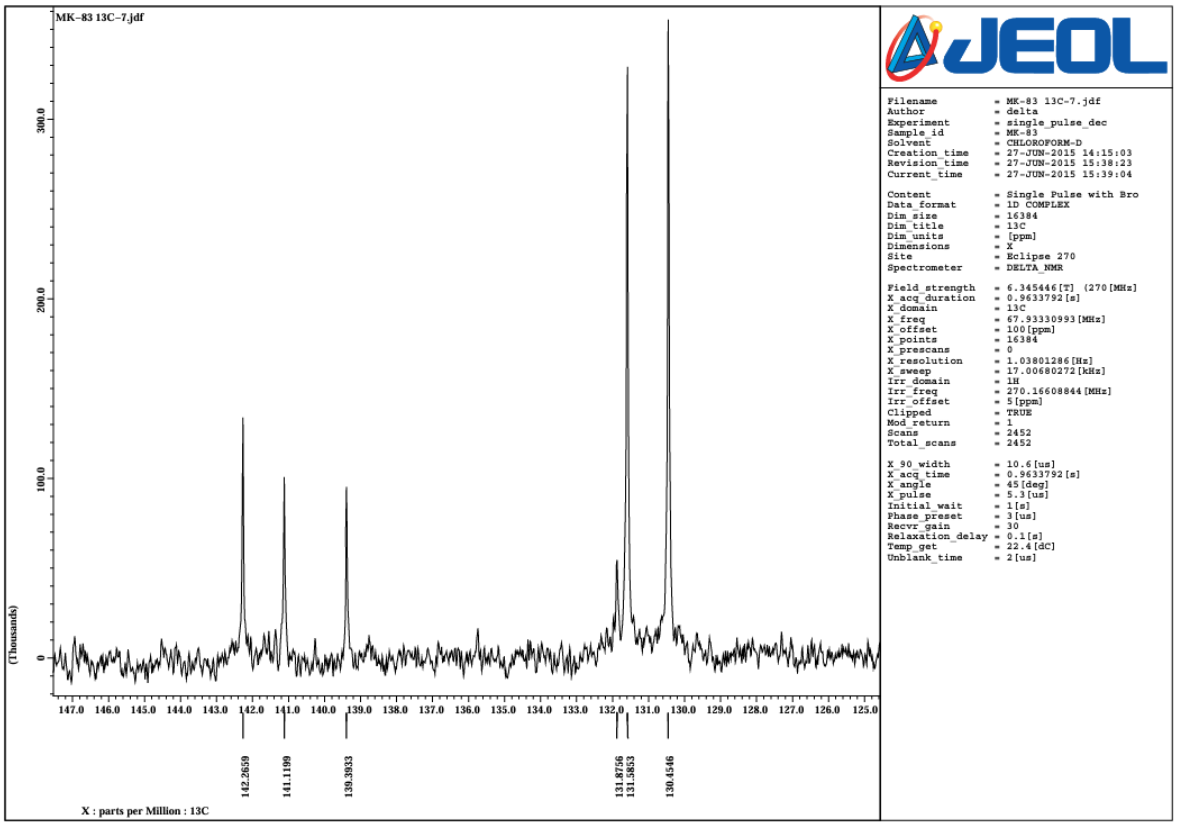

Fig. S37. Expanded aryl region of ^{13}C NMR spectrum of compound $Mes[CH_3(OH)CHC(O)CH_2]TeBr_2$ (**6**) in $CDCl_3$.

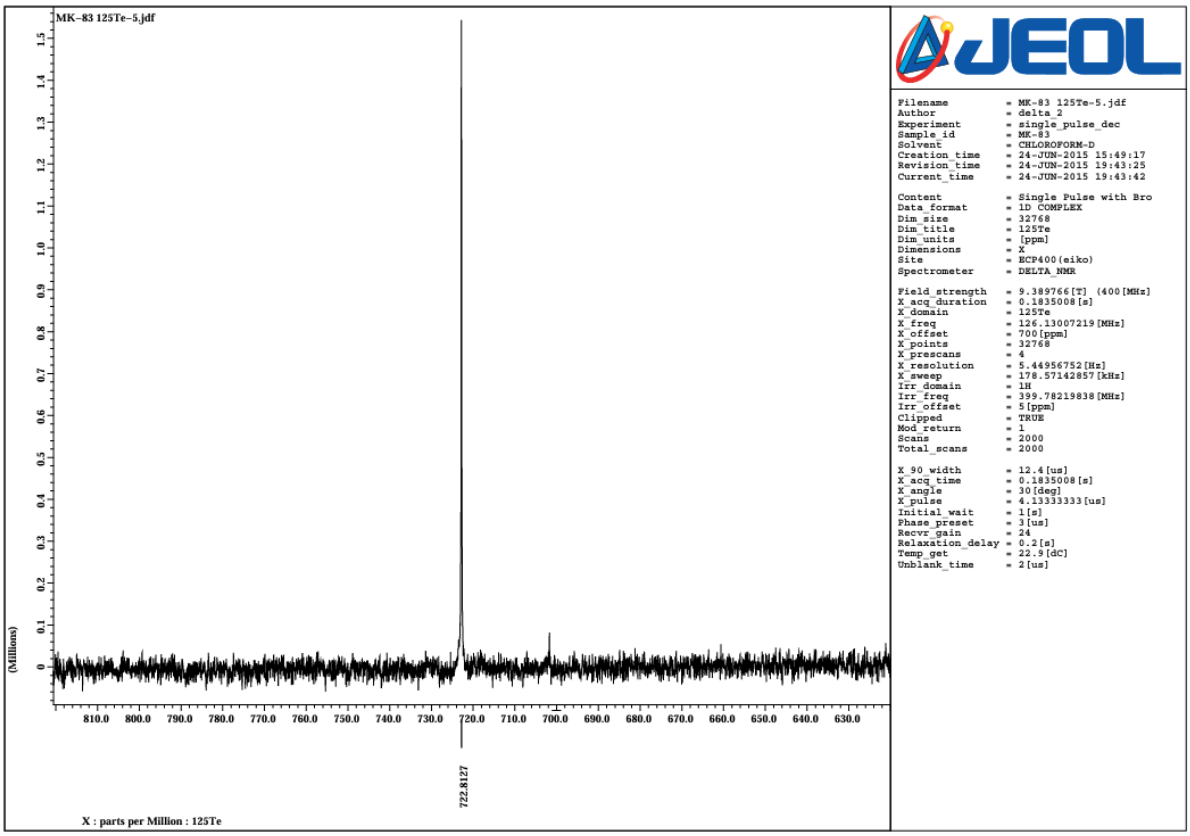

Fig. S38. ^{125}Te NMR spectrum of compound Mes[CH_3(OH)CHC(O)CH_2]$TeBr_2$ (**6**) in $CDCl_3$.